

Arnaud Dessein

Modelling distortion in condenser microphones

Master's Thesis, June 2009

Arnaud Dessein

Modelling distortion in condenser microphones

Master's Thesis, June 2009

A handwritten signature in black ink, consisting of a series of fluid, connected strokes that form a stylized name.

Modelling distortion in condenser microphones

This report was prepared by

Arnaud Dessein

Supervisors

Finn Jacobsen - DTU

Finn T. Agerkvist - DTU

Erling Sandermann Olsen - Brüel & Kjær

Anders Eriksen - Brüel & Kjær

External examiner

René Burmand Johannesson - Oticon

Department of Electrical Engineering
Centre for Electric Technology (CET)
Technical University of Denmark
Elektrovej building 325
DK-2800 Kgs. Lyngby
Denmark

www.elektro.dtu.dk/cet

Tel: (+45) 45 25 35 00

Fax: (+45) 45 88 61 11

E-mail: cet@elektro.dtu.dk

Release date: June 30th, 2009

Category: 1 (public)

Edition: Second - Corrected version edited after the oral presentation

Comments: This report is part of the requirements to achieve the Master of Science in Engineering (M.Sc.Eng.) at the Technical University of Denmark. This report represents 30 ECTS points.

Rights: ©Arnaud Dessein, 2009

Preface

In the scope of my studies at the Technical University of Denmark (DTU) in the Engineering Acoustics master program, I have done my final project about modelling distortion in condenser microphones. This subject was originally proposed by Brüel & Kjær Sound & Vibration Measurement A/S (B&K) under the title *Distortion process in condenser microphones*.

In February 2009 I have started my literature work at DTU for one and a half month. I have been able to gather and analyse about thirty documents related to my subject.

In mid-march 2009 I moved to Brüel & Kjær headquarters in Nærum in order to work on modelling the distortion. Starting with a very simple model, I have increased the complexity gradually in order to reach a model that gives satisfactory results.

This project has been very interesting and rewarding. It gave me the opportunity to apply my theoretical knowledge from DTU and make a five months internship in a leading company in acoustic transducers.

I would like to take this opportunity to thank my supervisors for their great help. In particular, I would like to thank Erling Sanderman Olesen for guiding me in my project and for all the time he spent answering my questions. Thanks to Erling Frederiksen for all the useful explanations he gave me. I would also like to thank all the others employees at Brüel & Kjær for their welcome and the very pleasant and stimulating atmosphere. Finally, I would like to thank Sébastien Tardy for rereading my report and Aude-Aline Sastre for her patience and understanding.

This report has been submitted the 26th of June 2009.

The defence of the master thesis took place at DTU the 2nd of July 2009.

Summary

Distortion in condenser microphones has different origins : electrical, acoustical and mechanical. According to the preliminar litterature study, the electrical distortion is found dominant compared to the acoustical and mechanical distortions. The electrical distortion is produced by two phenomenon. First, the presence of passive capacitances in parallel to the active capacitance (which varies with the acoustic signal) introduces nonlinearity in the transduction principle. Then, the curved deflection profile of the diaphragm is responsible for an inhomogeneous repartition of the active capacitance.

Many papers have already been written about the effect of stray (passive) capacitance but the influence of the deflection shape has not been studied into details yet.

A better prediction of the membrane deflection profile is made possible by a new model developped during this study. This model takes the variations of the electrostatic force along the membrane into account. When the movement of the membrane is large (high sound pressure levels or soft diaphragm microphones), these variations become an important factor in the detrmination of the deflection shape and thus in the microphone distortion.

The influence of the membrane deflection shape is then simulated using different models of membrane deflection. It is found that the influence of the curved deflection shape on the distortion is about 6 dB (re fundamental) for a normal measuring microphone and about 7 dB for a low-noise microphone (soft diaphragm).

Optimum backplate radius and reduction of the distortion by means of a curved backplate are investigated. A reduction of approximately 5 dB is found possible by using a curved backplate with an optimised radius of curvature.

Résumé

15 Mars 2017

Les origines de la distorsion dans les microphones électrostatiques sont multiples : électrique, acoustique et mécanique. Selon une étude bibliographique préliminaire, la distorsion électrique domine. Deux phénomènes sont responsables de la distorsion électrique. Tout d'abord, la présence de capacités en parallèle avec la capacité dite *active* (variant avec le signal acoustique) introduit une non-linéarité dans le principe de transduction. Ensuite, la membrane ayant un profil de déflexion courbé, la capacité active varie avec la position sur de la surface de la membrane.

Plusieurs articles concernant les effets des capacités parallèles ont été publiés, mais l'influence du profil de déflexion de la membrane n'a encore jamais été étudié en détails.

Une meilleure prédiction du profil de déflexion est rendue possible par un nouveau modèle, développé au cours de cette étude. Ce modèle prend en compte les variations de la force électrostatique le long de la membrane. Lorsque le mouvement transversal de la membrane est important (hauts niveaux de pression acoustique ou microphones à diaphragmes souples), ces variations deviennent un facteur important dans la détermination du profil de déflexion et par conséquent dans la distorsion produite par le microphone.

L'effet du profil de déflexion est simulé en utilisant différents modèles de déflexion. Il résulte de cette étude que le profil de déflexion est responsable de 6 dB de distorsion (par rapport au fondamental) dans le cas d'un microphone de mesure conventionnel et de 7 dB pour un microphone à bas bruit (diaphragme souple).

La taille optimale de l'armature fixe et la réduction de la distorsion au moyen d'une armature fixe à profil courbé sont étudiés. Une possible réduction d'environ 5 dB est prédite si un rayon de courbure optimum est utilisé pour le profil de l'armature fixe.

Contents

List of Figures	x
List of Tables	xii
Nomenclature	xv
1 Introduction	1
2 Introduction to condenser microphones	3
2.1 A short history	3
2.2 Principle	4
2.3 Polarisation	5
3 Theory and literature overview	7
3.1 Electrical distortion introduced by the preamplifier	7
3.2 Distortion in externally polarised condenser microphones . . .	8
3.2.1 Active and passive capacitances in a condenser microphone	9
3.2.2 Distortion due to the presence of stray capacitances .	11
3.2.3 Movement of the electrical charges and non-linear electrostatic forces	11
3.2.4 Considerations about the two causes of distortion . . .	13

3.3	Distortion in electret condenser microphones	13
3.4	Distortion in silicon condenser microphones	14
3.5	Methods for measuring distortion in condenser microphones .	15
3.6	Modelling distortion in condenser microphones	16
3.6.1	Finite element method	16
3.6.2	Nodal analysis	17
3.6.3	Membrane deflection calculation	18
4	Modelling the distortion	23
4.1	Determination of the edges capacitance	23
4.2	Determination of the membrane deflection	27
4.2.1	List of the forces acting on the membrane	29
4.2.2	Parabolic model	31
4.2.3	Two-regions model	32
4.2.4	N-regions model	36
4.3	Calculation of the output voltage and distortion	40
4.3.1	Output voltage	40
4.3.2	Distortion	41
5	Obtained results	43
5.1	Simulated microphones	44
5.1.1	Microphones data	44
5.1.2	Equivalent volume of the diaphragm	44
5.1.3	Adjustment of the model sensitivity	46
5.2	Predicted membrane deflection profile	46
5.2.1	Standard microphone B&K 4190	46
5.2.2	Low noise microphone B&K 4179	48
5.3	Predicted sensitivity	49
5.3.1	Standard microphone B&K 4190	49
5.3.2	Low noise microphone B&K 4179	49

5.4	Predicted distortion	51
5.4.1	Standard microphone B&K 4190	51
5.4.2	Low noise microphone B&K 4179	52
5.5	Influence of the diaphragm and backplate radius ratio on the distortion	53
5.6	Reducing distortion	53
6	Perspectives	59
7	Conclusion	61
	Bibliography	62

List of Figures

2.1	Sectional view of a condenser microphone cartridge	4
3.1	Schema of the different capacitances	9
4.1	Electric field simulated with COMSOL software (conductive backplate)	24
4.2	Electric field simulated with COMSOL software (dielectric backplate)	25
4.3	Schema for the calculation of the electrostatic distances	26
4.4	Sketch of the microphone	28
4.5	Restoring forces applied to a piece of membrane	30
4.6	Schema of the membrane split into $N=4$ segments	37
5.1	Predicted deflection of the microphone B&K 4190 exposed to 140 dB SPL	47
5.2	Predicted sensitivity of the microphone B&K 4190	50
5.3	Predicted sensitivity of the microphone B&K 4179	50
5.4	Predicted distortion of the microphone B&K 4190	51
5.5	Simulated distortion for the microphone B&K 4179	52
5.6	Influence of the backplate radius on the distortion (B&K 4190)	54
5.7	Influence of the backplate curvature radius on the distortion (B&K 4190)	55

5.8	Influence of V , h and Rc on the distortion (B&K 4190)	. . .	56
-----	--	-------	----

List of Tables

5.1	Parameters used for the simulation of the B&K microphones	45
5.2	Distance membrane backplate h used to obtain the correct sensitivity	46
5.3	Peak-peak deflection value of the B&K 4190 at 140 dB SPL .	49
5.4	Peak-peak deflection value of the B&K 4179 at 140 dB SPL .	49
5.5	Influence of the model on the distortion results (B&K 4190) .	51
5.6	Influence of the model on the distortion results (B&K 4179) .	53

Nomenclature

Sound pressure levels expressed in dB SPL are RMS values related to a pressure reference of 20 μPa .

Microphone sensitivities are calculated with the RMS value of the total microphone output voltage.

Distortion levels expressed in dB are RMS values related to the fundamental.

Greek letters

$\alpha(r)$	Deflection of the membrane in the α region	m
$\beta(r)$	Deflection of the membrane in the β region	m
ω	Radial frequency of the sound pressure signal	$\text{rad}\cdot\text{s}^{-1}$
ρ	Air density	$\text{kg}\cdot\text{m}^{-3}$
σ	Membrane tensile stress	Pa
τ	Membrane tension	$\text{N}\cdot\text{m}^{-1}$
ε_0	Absolute permittivity	$\text{A}\cdot\text{s}\cdot\text{V}^{-1}\cdot\text{m}^{-1}$

Roman letters

ΔC_a	Change of active capacitance	F
A	Condenser plates area	m^2
A_b	Total backplate area (including area of holes)	m^2

A_d	Area of the diaphragm	m^2
A_h	Area of holes in backplate	m^2
A_n	Amplitude of the n^{th} harmonic in the output voltage	V
C	Condenser capacitance	F
c	Speed of sound in the air	$\text{m}\cdot\text{s}^{-1}$
C_0	Static capacitance	F
C_a	Active capacitance	F
C_e	Edges capacitance	F
C_h	Housing capacitance	F
C_l	Load capacitance	F
C_p	Total passive capacitance	F
C_{0a}	Active part of the static capacitance	F
$C_{ad,eq}$	Total equivalent acoustic compliance of the diaphragm	$\text{m}^5\cdot\text{N}^{-1}$
C_{ad}	Acoustic compliance of the diaphragm alone	$\text{m}^5\cdot\text{N}^{-1}$
C_{md}	Mechanical compliance of the diaphragm	$\text{m}\cdot\text{N}^{-1}$
d	Distance between the two plates of a condenser	m
d_a	Effective electrostatic distance in the air	m
D_n	n^{th} harmonic distortion	
d_S	Effective electrostatic distance in the backplate support	m
d_s	Distance backplate-diaphragm when the diaphragm is at its static position	m
E	Output voltage of a capacitor or cartridge	V
E_0	Polarisation voltage (Frederiksen notation)	V
E_{eff}	RMS value of the total output voltage	V
E_{fm}	Output voltage of the condenser microphone (flat diaphragm model)	V
e_{peak}	Peak output voltage of the preamplifier	V
f_a	Acoustic force	N

F_e	Electrostatic force	N
F_r	Restoring force	N
f_r	Restoring force	N
h	Distance between the two plates of a condenser (or between the diaphragm and the backplate)	m
k	Spring constant	$\text{N}\cdot\text{m}^{-1}$
L_e	Total backplate border length	m
n	Harmonic order	
P	Total pressure acting on the membrane	Pa
p_0	Pressure of reference (1 Pa)	Pa
P_a	Acoustic pressure	Pa
P_e	Electrostatic pressure	Pa
Q	Charge stored in a capacitor	C
R	Radius of a circle	m
r	Position from the centre of the diaphragm	m
R_b	Radius of backplate	m
R_d	Radius of the diaphragm	m
R_S	Ratio of effective and total backplate	
S_c	Sensitivity of the cartridge	$\text{V}\cdot\text{Pa}^{-1}$
SPL_{peak}	Maximum SPL corresponding to the peak output voltage of the preamplifier	dB re 20 μPa
t	Time	s
t_d	Diaphragm thickness	m
u	Deflection of the membrane (positive towards the backplate)	m
u_0	Deflection at the centre of the diaphragm	m
u_b	Deflection of the membrane at $r = R_b$	m
V	Polarisation voltage	V
V_b	Volume of the back cavity	m^3

V_d	Equivalent volume of the diaphragm	m^3
V_f	Volume of air displaced by a flat diaphragm profile	m^3
V_p	Volume of air displaced by a parabolic diaphragm profile	m^3
W	Energy stored in a capacitor	J
W_b	Thickness of the backplate	m
y	Relative diaphragm displacement	
y_m	Amplitude of the relative diaphragm displacement	

Introduction

At low sound pressure levels, condenser microphones have a very low distortion and the distortion increases with the sound level in a known way. The causes of distortion have been investigated in different papers and theoretical ways to reduce it have been proposed.

The aim of this study is to realise a comprehensible understanding about distortion in condenser microphone and to analyse the importance of the different factors leading to distortion. Phenomena such as electrostatic forces, diaphragm deflection shape and capacitance distribution will be examined by mean of different models implemented in a MATLAB program created for the needs of the study.

To begin, a short introduction to condenser microphones is given. It presents the theoretical basics needed to understand the working principle of this kind of microphones.

A chapter devoted to an overview of the articles and books related to the subject follows. Causes of distortion in the different kinds of condenser microphones, methods used to measure this distortion and the available models are the remarkable subjects treated in the literature.

Three different models of membrane deflection used in this study are then presented. In this chapter the models are presented in a theoretical point of view. How the models are programed is explained briefly.

The following chapter presents the results obtained with different configurations. Each configuration corresponds to a different phenomenon responsible for distortion. The distortion results given by these models are compared

and analysed in order to evaluate the importance of each phenomenon in the global distortion levels.

The thesis ends with a chapter which proposes possible ways to continue the analysis.

Introduction to condenser microphones

Condenser microphones are used nowadays for recording or measurement. Compared to other types of microphones (electrodynamic or ribbon), these microphones have a flat response. Their sensitivity, measured in mV/Pa, is also very stable in time : the typical change is less than 1 dB in 5000 years [1]. These microphones are sometimes called *electrostatic microphones* as electrostatic charges are stored and are responsible for the changes of the output voltage. The condenser microphone is the only type of microphone that can be used for accurate measurements as the uncertainty is less than about 0.1 dB (1.0 %) over a wide range of audio frequencies [2, Ch.1].

2.1 A short history

The condenser microphone was invented by E. C. Wentz in 1917, some years after the development of the electronic amplifier. In the 1920's and 1930's, the condenser microphones manufactured by the Western Electric Company were the most used and became *de facto* the unofficial standard microphones for sound pressure measurements [2].

Later, it has been shown experimentally that the condenser microphone obeys the reciprocal theorem; this made it possible to improve the calibration of condenser microphones using the "reciprocity method" and use them during the years 1940-45 as primary reference standards.

The condenser microphone has been continually improved since the post-war years as new manufacturers used new materials for the diaphragm (stainless steel instead of duralium) and improved the characteristics (e.g. holes in the backplate in order to control the behaviour at the resonance frequency).

The material used for the housing and diaphragm support are also chosen carefully in order to reduce the influence of the temperature and relative humidity on the microphone sensitivity. Indeed, if the thermal coefficients of expansion of the different materials are too much different, the tension of the membrane is modified and consequently the sensitivity is affected.

2.2 Principle



Figure 2.1: Sectional view of a condenser microphone cartridge

The term *microphone* is usually used to name the combination of the cartridge (also called capsule) and the preamplifier. The cartridge is where the transduction occurs : the acoustic pressure signal is transformed into a variation of electrical voltage. The next stage is the preamplifier which converts the high output impedance of the cartridge (due to the polarisation resistance of $10\text{ G}\Omega$ approximately) to a sufficiently low output impedance to be transmitted through a cable [3, Ch.4].

The capsule is essentially made of two conductive plates placed very close to each other. One of these plates is the membrane of the microphone, the second one is the backplate. These two plates form a capacitor (often called *membrane-backplate capacitor*) which is polarised with a constant voltage applied through a large electrical resistance (the polarisation resistance mention above). The polarisation process injects a given amount of electric charges in the condenser. The variations of the sound pressure difference between the outside and the inside of the microphone make the membrane move back and forth. As this movement changes the distance

between the two plates, the capacitance of the condenser varies with the sound pressure. The electrical resistance is large enough (about $10\text{ G}\Omega$) to render the electrical current induced by the change of capacitance negligible, even at low frequencies. The value of the membrane-backplate capacitor is typically 15 pF [1], which means a time constant of 15 ms . Thus, the charge in the capacitor remains constant during measurement (down to $5\text{-}10\text{ Hz}$): the change of capacitance gives rise to a variation of the voltage across the condenser (the output voltage).

It is a common misunderstanding that this voltage is proportional to the change of capacitance [4], it is actually inversely proportional as

$$E = \frac{Q}{C} \quad (2.1)$$

where E , Q and C are respectively the output voltage, the charge (constant) and the capacitance. The output voltage is in fact proportional to the membrane displacement u as we have for a simple parallel plates condenser [5]:

$$C = \frac{\varepsilon_0 \cdot A}{h - u} \quad (2.2)$$

where A is the area of the plates (supposed of equal dimensions), h the distance between these two plates, u the deflection of the membrane (positive towards the backplate) and ε_0 the absolute permittivity. Then

$$E = \frac{Q \cdot (h - u)}{\varepsilon_0 \cdot A} \quad (2.3)$$

2.3 Polarisation

The polarisation of the cartridge can be done in two different ways, by external polarisation or by pre-polarised electret.

As explained in section 2.2, the external polarisation consists in applying a polarisation voltage through a very large resistor (a typical polarisation voltage is 200 V). Another technique of external polarisation exists [2, Ch.3] where the membrane-backplate capacitor is placed in a tuning circuit; the vibrations of the diaphragm result in the modulation of a high frequency carrier voltage. This solution which makes it possible to measure very low frequency signals, will not be discussed in this report.

On the other hand, the electret is a permanently charged thin polymer film put on one of the plates. Nowadays the electret is usually put on the backplate, a solution that makes it possible to separate the optimisation of the diaphragm and the electrical performances [5]. This solution is adopted in new Brüel & Kjær microphone designs [3].

As electret microphones do not require to be fed with high voltage, they are much more convenient for portable devices. The Brüel & Kjær pre-polarised microphones have an electret charged negatively which introduces an inversion of polarity (phase shift of 180°) compared with the externally polarised ones.

Theory and literature overview

Distortion in condenser microphones has been investigated for many years, the oldest paper found dates from 1976 [6] but there is a chance that investigations have been done even before this date.

The aim of this chapter is to provide an overview of the available literature about distortion in condenser microphones. Measuring methods, origins and models are presented. The most important origins are identified and an analysis method is chosen.

The approach and the method used in this study are presented in details. These choices, that have decided the orientation of this project, are justified and discussed.

3.1 Electrical distortion introduced by the preamplifier

As explained in the introduction to condenser microphones (chapter 2), the preamplifier is a necessary stage to convert the very high impedance of the cartridge to a low enough impedance to drive the lengths of cable until the amplifier or recorder. As the voltage at the output of the cartridge is already high (around the polarisation voltage in the case of externally polarised microphones), these amplifiers have usually a gain of unity or less.

In [7], two different kinds of amplifiers are presented : vacuum tube and solid-state topologies (based on field-effect transistors (FET)). In this pa-

per, the approach is based on an audio engineering point of view : the tube-transformers are appreciated for their sonic attributes. Undoubtedly this means an important 3rd harmonic distortion. The first topologies based on FETs appeared in the late 1960's. The available current for the FET was only 1 mA at that time¹, limiting severely the dynamic range of the microphone (up to 118 dB SPL). The solid-state topologies present lower distortion than vacuum tube. The drawback of FET topologies is the hard clipping : odd-harmonics are abruptly generated when the transistor is saturated.

Nowadays, preamplifiers are based on FET topologies. The maximum SPL can be calculated from the following equation (from [3, Ch.4]) :

$$SPL_{peak} = 94 + 20 \log \left(\frac{e_{peak}}{S_c \cdot p_0} \right) \quad (3.1)$$

where SPL_{peak} is the maximum SPL above which the preamplifier generates distortion, e_{peak} is the peak output voltage of the preamplifier, S_c is the sensitivity of the cartridge and p_0 is the pressure of reference (1 Pa).

According to the product data [1, 8], for a microphone made of a cartridge Brüel & Kjær 4190 (B&K 4190) polarised at 200 V and a preamplifier B&K 2669, the SPL_{peak} is :

$$SPL_{peak} = 94 + 20 \log \left(\frac{(200 - 10)/2}{50 \cdot 10^{-3} \cdot 1} \right) = 159.6 \text{ dB SPL} \quad (3.2)$$

According to the same product data, the distortion produced by the preamplifier under the limit of clipping is less than -80 dB (0.01%) (for the B&K 2629 at 1 kHz and 25 V out).

According to [3, Ch.4], the cartridge 4190 produces 3% (-30.5 dB) of distortion around 148 dB SPL. In conclusion, even at the highest levels measurable by the cartridge, the distortion of the preamplifier is completely negligible (300 times lower).

3.2 Distortion in externally polarised condenser microphones

In condenser microphones, the distortion can have different origins. As these sensors are transducers, meaning electroacoustic devices, one can consider three sources of distortion : electrical, mechanical and acoustical [9].

¹This current was provided by the phantom power. The limit of 1 mA was necessary to keep the voltage high enough for the polarisation of the cartridge

Mechanical and acoustical distortions are much less important than the electrical one; they are caused by the mechanical properties of the membrane, the air-damping and the stiffness of the cavity.

The electrical distortion is due to the non linearity of the transduction principle. This non linearity is caused by :

- the presence of passive capacitances in the cartridge,
- the curved membrane deflection profile.

3.2.1 Active and passive capacitances in a condenser microphone

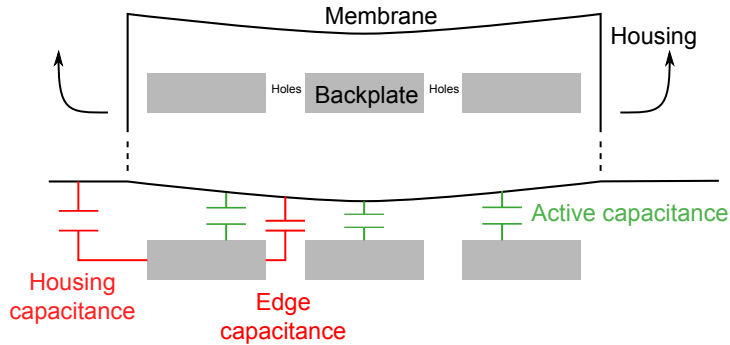


Figure 3.1: Schema of the different capacitances

3.2.1.1 Active and static capacitances

The active capacitance (in green on figure 3.1) varies with the sound pressure; it is responsible for the variations of the output voltage. The active capacitance is the capacitance of the membrane-backplate capacitor. It is calculated from the distance $d(r)$ between the diaphragm and the backplate as shown in equation (3.3) :

$$C_a = \iint_A \frac{\varepsilon_0}{d(r)} dA = \int_0^{R_b} \frac{2\pi r \varepsilon_0}{h - u(r)} dr \quad (3.3)$$

where C_a is the active capacitance, R_b the radius of backplate and r the position from the centre of the diaphragm.

The rest capacitance C_0 is a specific case of the active capacitance. It corresponds to the value of the active capacitance C_a when the diaphragm is at its rest position (the static deflection) : the microphone is polarised

but not exposed to any sound pressure. For a given polarisation voltage, C_0 is a constant; it depends on microphone parameters such as the diaphragm tension.

As one can see from equation (3.3), the profile $u(r)$ of the deflection above the backplate has an influence on the value of the active capacitance. The larger the static deflection, the larger the rest capacitance. The larger the deflection caused by the action of a sound pressure, the larger the active capacitance for this sound pressure.

3.2.1.2 The different kinds of passive capacitances

The passive capacitances (also called *stray* capacitances and in red on figure 3.1) are the capacitances that remain constant whatever the acoustic pressure. Three passive capacitances can be observed :

The housing capacitance corresponds to the capacitor created by the housing of the microphone and the backplate. Diaphragm and housing are electrically connected, meaning that electrostatic charges are also stored in the housing during the polarisation process. These charges can move from the housing (passive capacitance) to the diaphragm (active capacitance) during the excitation. The housing capacitance can be measured if the diaphragm is removed. For instance, the value of 1.65 pF has been measured for a microphone B&K 4190 by Brüel & Kjær.

The edges capacitance is caused by the holes in the backplate : these holes create additional conductive area facing the diaphragm. The effective distance between these surfaces and the diaphragm being much larger than the amplitude of the diaphragm vibration during the acoustic excitation, the variation of capacitance in the edges-membrane capacitor can be ignored.

The preamplifier capacitance is in fact the *load* capacitance (which explains the subscript l). It is the capacitance seen by the output of the cartridge. As a cartridge needs to be connected to a preamplifier (for polarisation and amplification of the output signal), it is assumed that the capacitance seen by the microphone is the input capacitance of the preamplifier. According to the product datasheet of a common preamplifier [8], the value of this capacitance does not exceed 0.45 pF. In this study the value 0.30 pF is used as a mean value².

²The input capacitance of most B&K preamplifiers is composed of two capacitances in parallel : the input capacitance of the preamplifier plus an additive capacitance of 0.2 pF used for the patented Charge injection Calibration Technique

The total passive capacitance C_p is the sum of the housing capacitance C_h , the preamplifier capacitance C_l and the edges capacitance C_e :

$$C_p = C_h + C_l + C_e \quad (3.4)$$

3.2.2 Distortion due to the presence of stray capacitances

Without any stray capacitance the output voltage would follow the expression :

$$E = V \frac{C_0}{C_a} \quad (3.5)$$

where V is the polarisation voltage and C_0 is the static capacitance.

Considering a plane capacitor, the active capacitance C_a is related to the deflection of the membrane by :

$$C_a = \frac{\varepsilon_0 \cdot A}{h - u} \quad (3.6)$$

then

$$E = V \frac{C_0}{\varepsilon_0 \cdot A} \cdot (h - u) \quad (3.7)$$

This last relation shows that in the absence of stray capacitance, the output voltage is proportional to the deflection and thus to the sound pressure (the restoring force is considered linear).

If passive capacitances are present in parallel to the active one, then the output voltage is :

$$E = V \frac{C_0 + C_p}{C_a + C_p} = V \frac{C_0 + C_p}{\varepsilon_0 \cdot A + (h - u) \cdot C_p} \cdot (h - u) \quad (3.8)$$

This relation is no longer linear : distortion is generated.

In other words, the passive capacitances behave as an additional constant capacitance in parallel to the active one. Without passive capacitance, the output voltage results in a compensation of two inversely linear relations; this compensation is disturbed if passive capacitances are present, leading to distortion [10]. The larger the ratio C_a/C_p , the weaker the influence of the passive capacitance and then the lower the distortion.

3.2.3 Movement of the electrical charges and non-linear electrostatic forces

As explained above, the housing and the diaphragm are electrically connected and the polarisation process stores a given amount of charges in

these two capacitors (diaphragm-backplate and housing-backplate). When the distance between the diaphragm and the backplate decreases under the influence of an acoustic pressure, the active capacitance increases. As the voltages across the two capacitors must remain equal (because they are connected), charges move from the passive to the active capacitance.

Moreover, one can see the active capacitance as an infinity of small active capacitances in parallel, each of these capacitance corresponding to a circular portion of the diaphragm³. Each capacitance is charged with an amount of electrical charges corresponding to the distance between the ring of diaphragm and the backplate. The charges can move from one active capacitance to another; as the deflection of the diaphragm is curved and more important in the centre, the amount of charges is more important in the middle than at the edges. This approach will be used later in this report for modelling the distortion. For the moment, it makes it possible to understand that the density of charge on the diaphragm is not constant.

In an isolated plane condenser (the charge inside the condenser is then constant in the time), the electrostatic force F_e acting on the diaphragm is constant :

$$F_e = -\frac{dW}{dd} \quad (3.9)$$

where F_e is the electrostatic force, W the energy stored in a capacitor and d the distance between the two plates of the condenser.

The energy stored in a condenser microphone can be expressed by :

$$W = \frac{1}{2} \frac{Q^2}{C} = \frac{C V^2}{2} \quad (3.10)$$

Using the first expression of W we get,

$$F_e = -\frac{Q^2 \varepsilon_0 A}{2} \quad (3.11)$$

It is true that the cartridge can be considered disconnected from the polarisation voltage source considering the time constant. But, because of the presence of passive capacitances, the charge in the active capacitance is *not* constant. Then, the active capacitance cannot be considered as being isolated.

The electrostatic force is then expressed using the second expression of W . For a plane condenser, the capacitance C is given by :

$$C(d) = \frac{\varepsilon_0 A}{d} \quad (3.12)$$

³Assuming axi-symmetric deflection profiles. This assumption is verified when the frequency of excitation is far below the first circular plate modes.

where A is the common area between the plates. Then it yields :

$$F_e = \frac{V^2 \epsilon A}{2 \cdot d^2} \quad (3.13)$$

As one can see, the relation between the electrostatic force and the deflection is not constant anymore and now non-linear. This makes the electrostatic force much stronger when the diaphragm is close to the backplate and the deflection profile asymmetric (regarding the static deflection).

Theoretically, the variations of electrostatic force over the membrane can be reduced and then the distortion by using a concave dished backplate. In 2002, Fletcher [11] wrote that a spherical concave dishing with a radius of curvature between about 1 and 2.5 m would lead to a reduction of the distortion, an increase of sensitivity and a larger maximum SPL. This will be simulated and examined in chapter 4.

If the change of active capacitance is made everywhere the same along the membrane, then the distribution of the forces is not changed. This is the case when the ratio of the distances membrane-backplate with and without sound pressure is everywhere the same. In the simple case of a plane condenser :

$$\Delta C_a = \frac{C_a}{C_{0a}} = \frac{\epsilon A_b}{d} \frac{d_s}{\epsilon A_b} = \frac{d_s}{d} \quad (3.14)$$

where ΔC_a is the change of active capacitance due to the sound pressure, C_{0a} the active part of the static capacitance and d_s the distance backplate-diaphragm when the diaphragm is at its static position.

3.2.4 Considerations about the two causes of distortion

In common microphones, the distortion produced by the transduction principle is more important than the one due to the non-linear electrostatic force. A model that only takes the stray capacitances into account is already a very good model to predict the distortion provided that the deflection of the membrane is not too large.

A more advanced model, taking the electrostatic forces into account is necessary to predict the distortion at very high levels or for microphones with soft diaphragms. These microphones are characterised by a very high sensitivity such as the B&K 4955, which has a sensitivity of 1.1 V/Pa [12].

3.3 Distortion in electret condenser microphones

In electret microphones, the polarisation of the condenser is done by a thin pre-polarised layer put on the backplate or (less usually) on the diaphragm.

The causes of distortion in prepolarised microphones are the same as in an externally polarised microphone : non-linearity in the physical parameters determining the movement of the diaphragm and presence of passive capacitances. However, the movement of the electrical charges in the electret is not perfectly known. Are the charges able to move as much as in an externally polarised backplate ? Since the electrostatic charges are stored differently, one could expect a different pattern for the harmonic distortion. According to [13] it appears that the increase of distortion with the sound pressure level follows the same pattern as the one observed with externally polarised microphones with no significant difference.

As explained in [5], the electret can be put on one side of a metallic diaphragm. Even if this technique is not often used nowadays, a study of the distortion produced in this kind of prepolarised microphones can be found in [14]. In this paper, Abuelma'atti explains that the preamplifier is not only necessary to convert the high impedance of the cartridge to a low output impedance but also to load the cartridge with a high impedance. Indeed, the distortion is shown to be related to the input impedance of the preamplifier : the distortion would be null in the case of an infinitely large resistance. It is also shown that the second harmonic distortion increases by 6 dB/octave and the third harmonic by 12 dB/octave (as explained below, these slopes are also observed in the case of externally polarised microphones). Finally, the physical dimensions of the electret are related to the distortion in a way that suggests that it is possible to optimise the electret microphones design to minimise harmonic distortion (for instance increasing the distance between the backplate and the electret when this one is at its rest position).

3.4 Distortion in silicon condenser microphones

Since 1983, micromachining techniques have been used to build miniature piezoelectric or piezoresistive microphones in silicon. More recent development is the fabrication of miniature silicon condenser microphones with an integrated field-effect transistor.

In order to reach the large sensitivity and the low noise level of conventional condenser microphones, it is necessary to use similar diaphragms with equal mechanical sensitivity. The consequence is a diaphragm movement which is as wide as in conventional condenser microphones having air gaps of 15 - 30 μm . The relative deflection is then much higher and then the distortion.

The causes of distortion are the same as in conventional microphones : non-linear and non-uniform electrostatic forces leading to an asymmetric dynamic deflection. Silicon microphones are also subject to passive capaci-

tance due to the bond pad⁴ and to the input capacitance of the preamplifier [15]. The edges of the membrane, where the movement is the smallest, act as a capacitance loading the active one. The influence of this less active capacitance can be reduced by reducing the size of the backplate. This source of distortion will be explained in details in the next sections as the principle is the same in normal size condenser microphones.

In 1997, Pedersen [16] did a study on harmonic distortion in silicon condenser microphones. In this paper, the author compares the results obtained with his model and the ones obtained theoretically. Both sets of results are in very good agreement. As expected, the levels of distortion are much higher than for conventional condenser microphone : 1% of distortion is reached around 110 dB SPL.

Another limitation of this kind of microphone is the maximum sound pressure level : the backplate is so thin that it can move back and forth. This behaviour reduces the collapse voltage and thus the maximum sound pressure the microphone can support [17].

A more advanced and theoretical approach is proposed by Abuelma'atti in [18]. Because the silicon condenser microphones are beyond the scope of this study, the content of this paper will not be detailed here.

3.5 Methods for measuring distortion in condenser microphones

Measuring distortion consists in generating a sound pressure field in front of a microphone and measuring the distortion in the electric signal generated by the transducer.

In general, the distortion produced by a condenser microphone is very low (less than 1% under 140 dB SPL [1]), then the device generating the sound pressure excitation must be free of distortion in this extent. Brüel & Kjær has developed two devices that makes it possible to measure the distortion of microphones.

The High Pressure Calibrator Type 4221 can be used to measure harmonic and intermodulation distortion up to 164 dB SPL in a wide frequency range (from 0.01 Hz to 1 kHz using couplers). The sound pressure is generated by a piston moved by an electrodynamic exciter; contrary to devices such as a pistonphone that produces constant volume displacement, this device is force-controlled. This makes the generated sound pressure independent from atmospheric pressure variations and change from adiabatic to isothermic

⁴The bond pad is a flat surface on which components are soldered.

conditions at low frequencies [19]. This device is no longer produced as it has been replaced a modern one able to reach higher levels : the 9719.

The automated high-pressure measurement system Type 9719 makes it possible to measure distortion up to 174 dB SPL at a single frequency (500 Hz) [20]. This device is based on a normal loudspeaker and a combination of resonating tubes that eliminates the generated distortion components in the sound field before it reaches the microphone under test. As the operating frequency is 500 Hz, three tubes are tuned at 500, 1000 and 1500 Hz respectively. The first tube reduces the displacement of the loudspeaker diaphragm (and then the generated distortion), the two others cancel the second and third harmonics. Moreover, the system is designed so as to reduce the vibrations transmitted to the microphone; indeed, high pressure microphones often have large moving mass and thus are very sensitive to vibrations. The generated sound field has a second-harmonic distortion of -16 dB and a third-harmonic distortion of -18 dB (relative to the level of the fundamental). The device has two build-in high pressure reference microphones, the results of their measurements are compared to the results from the microphone under test [21]. The uncertainty on the measurement of the RMS distortion is 0.05 dB below 164 dB SPL and 0.07 dB at 170 dB SPL.

3.6 Modelling distortion in condenser microphones

3.6.1 Finite element method

In [22], the finite element method is used to simulate the deflection of the membrane. The geometry of the model uses a circular arc to describe the membrane deflection shape. This choice, necessary for software capabilities, is justified : the real deflection shape (described by means of a Bessel function) is compared to a parabolic shape approximation and to a circular arc approximation; the differences are judged small enough.

The determination of the rest capacitance is done by finding the static deflection by force equilibrium. In order to determine the electrostatic force, the author approximates the derivative of the membrane-backplate capacitance with respect to the distance between these two plates by a second-order polynomial. The restoring force being linear and of the first degree, solving the equilibrium of the forces is then equivalent to finding the roots of a polynomial of the second order.

In order to describe the deflection of the membrane during operation, the electrostatic force in the case of constant charge (isolated capacitor) is also investigated. A third-order polynomial is used to approach the variation of the inverse of the active capacitance with the membrane deflection. As

the derivative of this quantity is needed in the expression of the electrostatic force in the case of an isolated capacitor, the third-order polynomial is easily differentiated. Solving the equilibrium of the forces is once again equivalent to finding the roots of a polynomial of the second order.

3.6.2 Nodal analysis

Nodal analysis is often used in electrical engineering to solve for the voltages and currents at any point in a circuit [23]. Thanks to electrical analogies, electroacoustic or mechanical systems can be modelled as electrical circuits and simulated by a program based on nodal analysis (e.g. SPICE).

According to Chen et al. [24], the polarisation of the capsule and the damping introduced by the holes in the backplate alters the lumped element parameters. In the same paper the authors present a lumped element model : the expression of the effective mass, compliance, resistance in the air gap, resistance in the acoustic holes, stiffness of the back chamber are found from energy considerations. The lumped pressure force and electrostatic force are also determined by the same means. The combination of these different lumped elements and forces leads to the equation of motion of the diaphragm and the capacitance is calculated using equation (3.3).

A model for edges capacitance is also proposed in this paper : as explained in details in the corresponding section in the modelling chapter (section 4.1), the curvature of the membrane can be neglected in the calculation of the edges capacitance. The authors have made the choice to introduce the backplate holes effect by means of an equivalent permittivity. The equivalent permittivity, function of the air gap thickness, is written as a third-order polynomial which coefficients are determined by numerical calculation. The model results are in good agreement with both the microphone noise and sensitivity measurements.

Michal Vlk has published two papers related to SPICE simulation of electrostatic transducers [25, 26]. The non-linear electrostatic force can be modelled by means of a non-linear admittance type fourpole. The movement of the membrane is assumed piston-like on the consideration that the compliance of the diaphragm is much larger than the one of the air gap. It is shown that the distortion predicted by the model is dependant on the pressure signal amplitude but also on the load resistance. The influence of the parallel capacitance (taken into account in the model) is unfortunately not analysed.

3.6.3 Membrane deflection calculation

In [10], Frederiksen proposes two models of distortion in condenser microphones. These models only take the major cause of the transduction principle non-linearity : the passive capacitances.

1. The first one corresponds to the most basic model possible : two flat plates parallel to each other, one being the backplate and the other the diaphragm, moving back and forth as a piston.
2. The second model is an improvement of the first one as the deflection is considered parabolic (it will be shown later that this assumption is reasonable).

3.6.3.1 Flat diaphragm displacement mode

In this model the membrane remains flat, the active capacitance C_a is the one of a plane capacitor given by the following equation derived from [10] :

$$C_a = R_S \frac{\varepsilon \pi R_b^2}{h - u} = C_0 (1 - y)^{-1} \quad (3.15)$$

where y is the relative diaphragm displacement and R_S the ratio of effective and total backplate defined by :

$$R_S = \frac{A_b - A_h}{A_b} \quad \text{and} \quad y = \frac{u}{h} = y_m \sin(\omega t) \quad (3.16)$$

where A_b is the total backplate area (including area of holes) and A_h is the area of holes in backplate.

If the total passive capacitance C_p is taken into account, the output voltage E is given by :

$$E = E_0 \cdot \frac{C_0 + C_p}{C_a + C_p} \quad (3.17)$$

where E_0 is the notation used by Frederiksen for the polarisation voltage.

Inserting (3.15) in (3.17) gives the expression of the output voltage E_{fm} of the microphone with a flat diaphragm mode :

$$\begin{aligned} E_{fm} &= E_0 \cdot \frac{C_0 + C_p}{C_0 \cdot (1 - y)^{-1} + C_p} \\ &= E_0 - E_0 \cdot \frac{C_0}{C_0 + C_p} \left(y - \left(\frac{C_p}{C_0 + C_p} \right)^1 \cdot y^2 + \left(\frac{C_p}{C_0 + C_p} \right)^2 \cdot y^3 - \dots \right) \\ E_{fm} &= E_0 - E_0 \cdot \frac{C_0}{C_0 + C_p} (y + F_2 \cdot y^2 + F_3 \cdot y^3 + \dots) \end{aligned} \quad (3.18)$$

where the constant F_n of the n^{th} harmonic is :

$$F_n = \left(-\frac{C_p}{C_0 + C_p} \right)^{n-1} \quad (3.19)$$

Equation (3.18) easily yields to the expression of the n^{th} harmonic distortion component D_n :

$$D_n = \left(\frac{y_m}{2} \cdot \frac{C_p}{C_0 + C_p} \right)^{n-1} \cdot 100\% \quad (3.20)$$

but this can be rewritten using equation (3.19) for latter comparison :

$$D_n = \left(\frac{y_m}{2} \right)^{n-1} \cdot |F_n| \cdot 100\% \quad (3.21)$$

The distortion decreases with the order n and when the passive capacitance C_p decreases.

Note that in the ideal case where there is no stray capacitance, the electrical distortion of the flat diaphragm microphone would be zero.

The factor $\left(\frac{y_m}{2}\right)^{n-1}$ in equation (3.21) means that the n^{th} harmonic distortion component increases with the amplitude of the signal at the power $n - 1$. On a graph where the harmonic distortions are plotted as a function of the sound pressure level (both magnitude in dB scale), the graph corresponding to the second harmonic distortion increases linearly with a slope of +1 dB/dB_{SPL} and the third harmonic distortion with a slope of +2 dB/dB_{SPL}.

3.6.3.2 Parabolic deflection profile

In this model, the deflection $u(r)$ of the microphone membrane is assumed parabolic :

$$u(r) = u_0 \left(1 - \frac{r^2}{R_d^2} \right) \quad (3.22)$$

where u_0 is the deflection at the centre of the diaphragm of radius R_d .

This is a better description of the membrane deflection as the true deflection is described by a Bessel function of the first kind and 0th order. This model leads to a better estimation of the active capacitance : the movement of the membrane borders is smaller than the movement at the centre. This means that the change in active capacitance is more important in the middle than on the borders. The borders are *less active* than the centre : the outer regions of the circular diaphragm act as a capacitance loading the active capacitance. The ratio C_a/C_p is reduced and then the distortion increased.

In other words, the first model based on a flat diaphragm profile overestimates the active capacitance and thus underestimates the distortion.

Frederiksen shows that the active capacitance C_a is then given by :

$$C_a = R_S \int_0^{R_b} \frac{\varepsilon \cdot 2 \cdot \pi \cdot r}{h - u(r)} dr \quad (3.23)$$

$$= R_S \int_0^{R_b} \frac{\varepsilon \cdot 2 \cdot \pi \cdot r}{h - u_0 \cdot \left(1 - \frac{r^2}{R_d^2}\right)} dr \quad (3.24)$$

$$C_a = C_0 \cdot (k - 1)^{-1} \cdot y_0^{-1} \cdot \ln \frac{1 - y_0}{1 - k \cdot y_0} \quad (3.25)$$

where $C_0 = R_S \frac{\varepsilon \cdot \pi \cdot R_b^2}{D}$, $R_S = \frac{A_b - A_h}{A_b}$, $k = 1 - \frac{R_b^2}{R_d^2}$ and $y_0 = \frac{u_0}{h}$. Inserting (3.25) in (3.17) gives the expression of the output voltage E_{pm} of the microphone with a parabolic diaphragm mode :

$$\begin{aligned} E_{pm} &= E_0 \cdot \frac{C_0 + C_p}{C_0 \cdot (k - 1)^{-1} \cdot y_0^{-1} \cdot \ln \frac{1 - y_0}{1 - k \cdot y_0} + C_p} \\ &= E_0 - E_0 \cdot \frac{k + 1}{2} \cdot \frac{C_0}{C_0 + C_p} \cdot (y_0 + F_2 \cdot y_0^2 + F_3 \cdot y_0^3 + \dots) \end{aligned} \quad (3.26)$$

where

$$F_2 = -\frac{C_0 \cdot (k^2 - 2 \cdot k + 1) + 4 \cdot C_p \cdot (k^2 + k + 1)}{6 \cdot (C_0 + C_p) \cdot (k + 1)} \quad (3.27)$$

and

$$F_3 = \frac{(C_0^2 + 4 \cdot C_0 \cdot C_p) \cdot (k^2 - 2 \cdot k + 1) + 6 \cdot C_p^2 \cdot (k^2 + 1)}{12 \cdot (C_0 + C_p)^2} \quad (3.28)$$

As before, the n^{th} harmonic distortion component is given by the equation (3.21), using the expressions of F_n given for this model.

As one can see, the distortion is a function of the parameter k : if the radius of backplate is reduced compared to the one of the diaphragm, the distortion decreases. As explained before, the less active capacitances on the border participates in the distortion. Reducing the radius of the backplate reduces their influence.

On the other hand, the reduction of the backplate leads to a reduction of the ratio C_a/C_p and thus to an increase of the distortion. A compromise should be found. The optimum value is given in [2] : the radius of the diaphragm should be $(2/3)^{1/2}$ times larger than the radius of the backplate.

3.6.3.3 Two-regions model

As explained in the previous section, the radius of the backplate should be smaller than the radius of the diaphragm.

The aim of this model is to take the electrostatic forces into account. If the backplate does not cover the entire diaphragm that means that the outer regions (from the circumference of the backplate to the edges of the diaphragm) are not exposed to any electrostatic force. It is then necessary to use a different set of equations to describe the deflection profile of this portion of diaphragm.

This model is described into details in the next chapter as it has been used and therefore programmed.

Modelling the distortion

The study presented in this report focuses on the low frequencies, where the microphone is spring-controlled. The mass and bending stiffness of the diaphragm are ignored. The movement of the membrane is assumed quasi static.

In these conditions, two models have been selected from the literature and one developed for the needs of the study. A model to calculate the edges capacitance has also been developed. After a presentation of this model of edges capacitance, the three models of membrane deflection (and then deflection) will be presented.

4.1 Determination of the edges capacitance

The active capacitance is the capacitance between the top surface of the backplate and the diaphragm. The backplate presents other surfaces (as the edges and the inside of the holes) that create unwanted capacitances. Even if the edge capacitance is a function of the distance membrane-backplate, the variation of this distance can be neglected and the edges capacitances considered passive.

The backplate edges and the diaphragm form two plates of a condenser. These two plates being perpendicular to each other, the distance between the two plates is not constant and depends on the position of a point running along the backplate. The capacitance depends on the effective distance between the two plates, it is not the geometrical distance but the one along

the electric field. It is then necessary to make a simulation of the electric field to know how this one is laid out.

Two different finite element models have been done using COMSOL software. The first model, shown on figure 4.1 corresponds to a conductive backplate, the second model shown on figure 4.2 corresponds to a dielectric backplate. On the latter model, the backplate is only a thin metallic layer put on the top of a ceramic support. The relative permittivity of the material constituting the support is $\varepsilon_r = 2$.

Model 1. As one can see on the right part of the figure 4.1 (the hole), the lines are almost perfectly circular with a radius of $h + z$, z representing the depth of a running point along the edge. This assumption is valid in the region where the electric field is strong enough to have an influence. The length of each line being

$$d_a(z) = \frac{\pi}{2}(h + z) \quad (4.1)$$

where d_a is the effective electrostatic distance in the air (subscript a standing for *air*), it is possible to calculate the capacitance between the two plates. The area is calculated considering the sum of the backplate holes perimeter

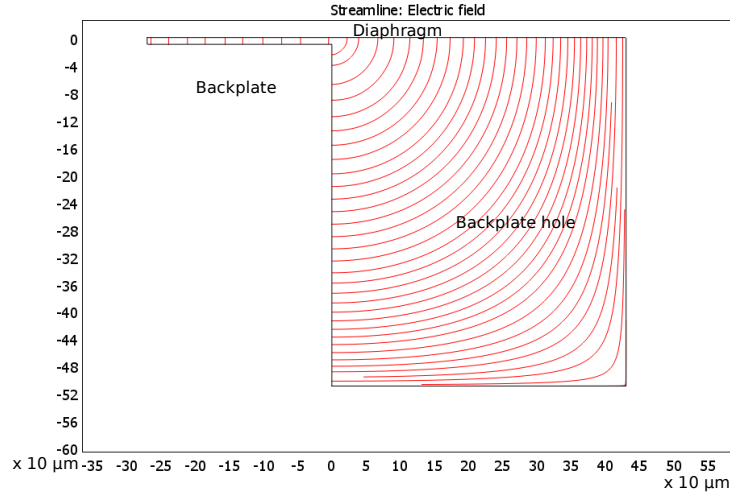


Figure 4.1: Electric field simulated with COMSOL software (conductive backplate)

plus the perimeter of the backplate itself. This length L_e is the total border length, multiplied with z it gives the running area. The integration is done

from $z = h$ to $h + W_b$.

$$\begin{aligned} C_e &= \int_h^{h+W_b} \frac{\varepsilon_0 L_e z}{\frac{\pi}{2}(h+z)} dz \\ &= \frac{2\varepsilon_0 L_e}{\pi} \left(W_b - h \cdot \ln \left[1 + \frac{W_b}{2h} \right] \right) \end{aligned} \quad (4.2)$$

where W_b is the thickness of the backplate and L_e its total border length.

Model 2. In this model the electric field lines are going through the support of dielectric constant ε_2 . In the support, the lines can be approximated by circular arcs where the electrical field is the strongest, meaning close to the diaphragm.

In order to determine the length of these arcs, their centre and radius should be calculated first. As one can see on figure 4.2 obtained by COMSOL simulation, all the lines are perpendicular to the bottom part of the layered backplate. Then, the centre of each arcs is at the same level as the bottom of the layer. In figure 4.3, the centre has the coordinates (X_c, Z_c) : the previous considerations yields to $Z_c = 0$.

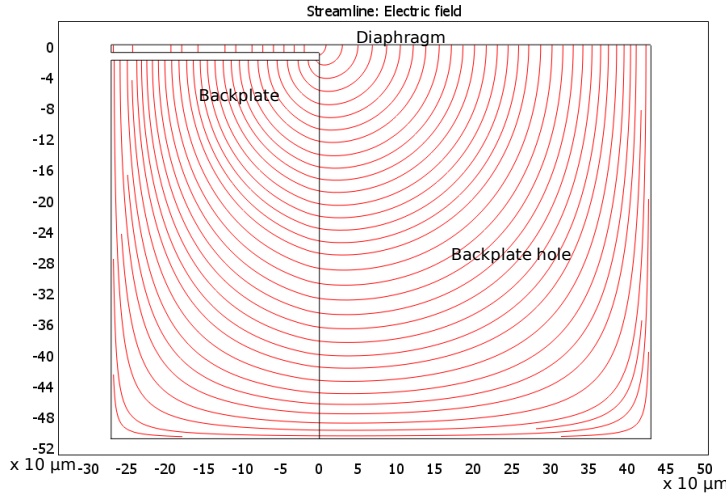


Figure 4.2: Electric field simulated with COMSOL software (dielectric backplate)

The points (x, z) of the arc in the support region follow the equation of a circle of centre C and radius R :

$$(x - X_c)^2 + z^2 = R^2 \quad (4.3)$$

The evaluation of this equation at point $A(a, 0)$ and $B(0, b)$ gives:

$$(a - X_c)^2 = R^2 \quad \text{at point A} \quad (4.4)$$

$$X_c^2 + b^2 = R^2 \quad \text{at point B} \quad (4.5)$$

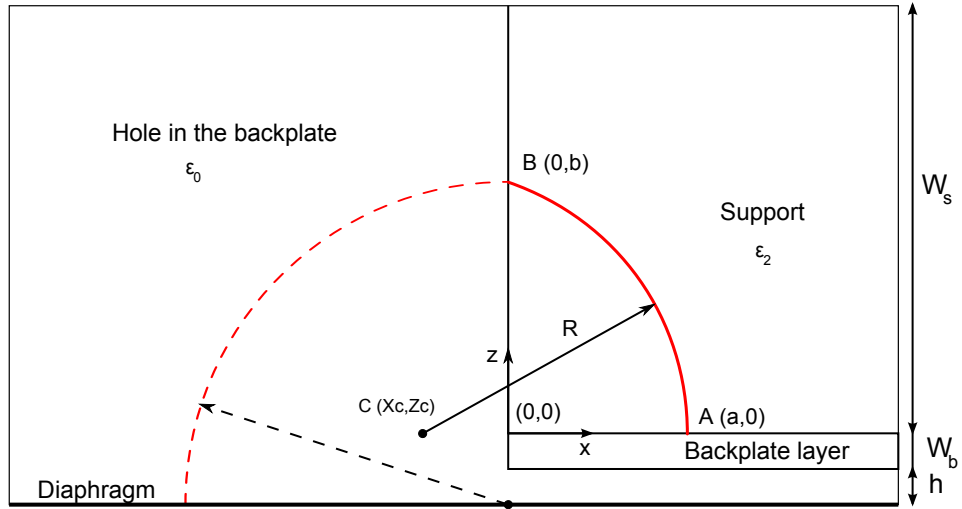


Figure 4.3: Schema for the calculation of the electrostatic distances

The difference (4.4) minus (4.5) leads to :

$$a^2 - b^2 - 2aX_c = 0 \quad (4.6)$$

$$X_c = \frac{a^2 - b^2}{2a} \quad (4.7)$$

Using $\alpha = \frac{a}{b}$ gives :

$$X_c = \frac{b}{2} \frac{\alpha^2 - 1}{\alpha} \quad (4.8)$$

On figure 4.2, the ratio $\alpha = \frac{a}{b}$ has been calculated for each arcs. This value has been found constant in the region of interest : $\alpha \approx 0.73$.

On one hand, the radius R of an arc is given by Pythagoras relation

$$R = \sqrt{X_c^2 + b^2} \quad (4.9)$$

On the other hand the angle $\beta = \widehat{ACB}$ between the points A and B is

$$\beta = \arctan\left(\frac{b}{|X_c|}\right) \quad (4.10)$$

thus the length $d_S(b)$ of an arc in the support is :

$$d_S(b) = \arctan\left(\frac{b}{|X_c|}\right) \sqrt{X_c^2 + b^2} \quad (4.11)$$

where d_S is the effective electrostatic distance in the backplate support. Simplifying this equation and using the variable z instead of b leads to :

$$d_S(z) = \arctan\left(\frac{2\alpha}{|\alpha^2 - 1|}\right) \sqrt{X_c^2 + z^2} \quad \text{with} \quad X_c = \frac{z}{2} \frac{\alpha^2 - 1}{\alpha} \quad (4.12)$$

Using equation (4.2) for the region from $z = h$ to $h = h + W_b$, the edge capacitance can be calculated by :

$$\begin{aligned} C_e &= \int_h^{h+W_b} \frac{\varepsilon_0 L_e z}{d_a(z)} dz + \int_{h+W_b}^{h+W_b+W_s} \left(\frac{\varepsilon_0 L_e z}{d_a(z)} + \frac{\varepsilon_2 L_e z}{d_S(z)} \right) dz \\ &= \int_h^{h+W_b+W_s} \frac{\varepsilon_0 L_e z}{d_a(z)} dz + \int_{h+W_b}^{h+W_b+W_s} \frac{\varepsilon_2 L_e z}{d_S(z)} dz \end{aligned} \quad (4.13)$$

4.2 Determination of the membrane deflection

The deflection shape of the membrane depends on many parameters such as the sound pressure, the size of the backplate and the polarisation voltage.

Only axi-symmetric deflection profile will be considered here. Thus the considerations on the deflection profile will be done on a section of the membrane, from its centre ($r = 0$) to its edge $r = R_d$. The entire geometry of the membrane can be created by a revolution of this curve (2π rotation angle).

Three forces are applied on the membrane (the expression of these forces will be given in details later) :

- The electrostatic force,
- the acoustic pressure force,
- the restoring force (spring force).

As the electrostatic force is only applied to the portion of membrane that faces the backplate, two concentric regions on the diaphragm should be considered as shown in figure 4.4 :

The β region is a circular region that extends from the centre to a distance equal to the backplate radius ($r = R_b$). On this region the membrane is exposed to the acoustic pressure, the electrostatic force and the restoring force.

The α region is an annular region that extends from $r = R_b$ to the edge of the diaphragm ($r = R_d$). On this region, only the acoustic pressure and the restoring force remain.

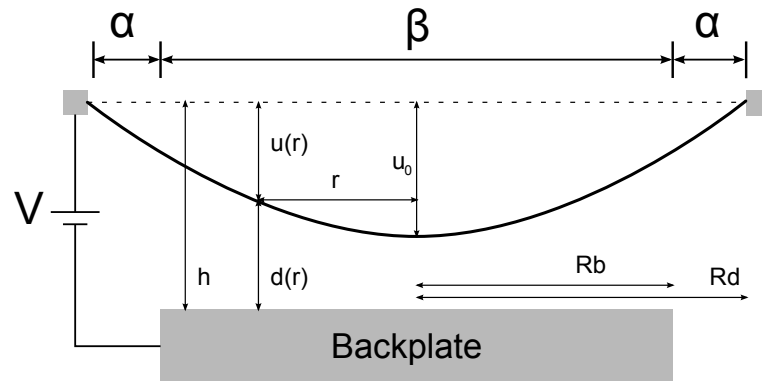


Figure 4.4: Sketch of the microphone

Three models of increasing complexity will be presented. Each model makes it possible to determine the deflections with and without sound pressure. What differs between these three models is the expression of the electrostatic force.

1. The first model considers that the electrostatic force is the same everywhere on the diaphragm. As shown below, this assumption leads to a parabolic deflection of the membrane. This model is good enough for small deflections (low SPL or very stiff diaphragm)
2. The second model uses two different functions to describe the deflection (one of the α region and one for the β region). This is a more realistic model when the radius of the backplate is smaller than the one of the diaphragm. On the β region, the electrostatic is still homogeneous. This model is a necessary transition between the first model and the third one.
3. The third model is an improvement of the second one as the electrostatic force in the β region depends on the position on the membrane. This is done by splitting the β region into pieces, the distance membrane-backplate (and thus the value of the electrostatic force) is evaluated for each segment. The deflection profile is no longer forced to take a parabolic shape. The electrostatic force distribution is then much more realistic. This model is adapted for high sound pressure or soft diaphragms.

The results of the three models will be presented and the improvements discussed : as the computation time is increasing with the complexity of the model, it could be important to be able to choose a faster algorithm when possible.

Every model is based on two steps :

1. During the charge of the condenser microphone (just after the preamplifier has been switched on), the applied voltage is constant and the amount of charges inside the condenser increases (these charges are provided by the polarisation source). During this period, the membrane deflects toward the backplate until it reaches a rest position called *static deflection*. Once this position is reached, two parameters are of interest : the total stored charge Q and the rest capacitance C_0 .
2. Once the condenser is charged, the time constant of the microphone is large enough to consider that there is no charge exchange between the microphone and the source anymore : the condenser can be considered as “disconnected” from the polarisation source. The charge in the condenser (defined by the static deflection) will remain constant. If a sound pressure is applied on the diaphragm, the membrane will reach a new equilibrium deflection. This deflection will change the active capacitance. The output voltage is then given by the ratio of the charge and the sum of the passive and active capacitance.

The second step is repeated with a new value of the sound pressure, following a sinusoidal excitation during four periods.

4.2.1 List of the forces acting on the membrane

General expressions of the forces¹ applied on the membrane will be given. Then, for each model, the expression of the electrostatic force is adapted.

4.2.1.1 The pressure force

The pressure force is due to the acoustic pressure acting on the diaphragm. This force is the same whatever the model,

$$f_a = P_a dA = P_a 2\pi r dr \quad (4.14)$$

where f_a and P_a are respectively the acoustic force and the acoustic pressure.

4.2.1.2 The restoring force

The tension τ of the membrane creates a restoring force f_r opposed to the deflection. As shown in figure 4.5 the action of the tension on the ring

¹In models 2 and 3, pressures are used instead of forces.

element can be represented by two forces f_1 and f_2 . As the bending stiffness is neglected, the forces are tangential. Moreover the displacement of the ring element is supposed only in the vertical direction, thus the horizontal components f_{1x} and f_{2x} compensate each other. f_{1y} and f_{2y} can be expressed

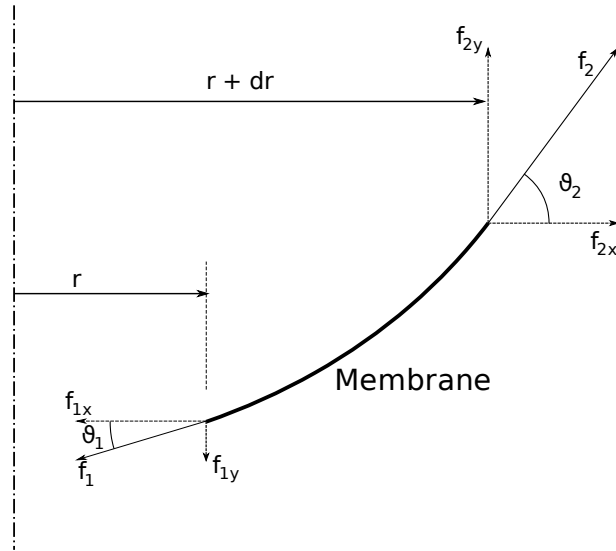


Figure 4.5: Restoring forces applied to a piece of membrane

as follow :

$$f_{1y} = f_1 \sin(\theta_1) \approx -f_1 \frac{du}{dr} \approx -2\pi r \tau \frac{du}{dr} \quad (4.15)$$

$$f_{2y} = f_1 + df_{1y} \approx -2\pi r \tau \frac{du}{dr} - 2\pi \tau d\left(r \frac{du}{dr}\right) \quad (4.16)$$

Thus :

$$f_r(r) = f_{1y} - f_{2y} = 2\pi \tau d\left(r \frac{du}{dr}\right) \quad (4.17)$$

4.2.1.3 The electrostatic force

Considering an infinitely small portion of membrane, this one is locally approximated parallel to the backplate. Then all the considerations about the electrostatic forces will be done on a plane condenser.

As explained in section 3.2.3, the electrostatic force in a plane condenser has a different expression whether the voltage between the two plates is constant or the charge stored in the condenser is constant.

- Constant voltage means that charges can come in or leave the plates. If the distance between the two plates varies, the charge changes in

order to keep the voltage constant. This condition requires a source of charges.

- Constant charge means that no charge can leave the condenser. If the distance between the two plates varies, then the output voltage changes.

Even though it has been mentioned that the time constant is so large that the cartridge can be assumed isolated from the polarisation source (meaning the total charge in the capsule is constant), the constant voltage condition is used for modelling the active capacitance. This means that the charge stored in the active capacitance varies. The active capacitance is not electrically isolated because the stray capacitances play the role of charge providers. Moreover, the active capacitance can be seen as an infinity of small active capacitances in parallel², meaning that the voltage across all of them is the same and that the charges can move from one active capacitance to another. In other words, the charges are moving in the membrane and thus are spread unequally (more charges in the centre); the overall charge is constant but the charge stored in the active capacitance is not.

The electrostatic force F_e in a capacitor which plates are spaced by a distance d has already been given in relation (3.13), page 13 :

$$F_e = \frac{E^2 \varepsilon A}{2 \cdot d^2} \quad (4.18)$$

Note that E is used instead of V , because in a charged condenser microphone the electrostatic force is proportional to the output voltage, not the polarisation voltage. During the polarisation process, V should be used in order to determine the static deflection. The fact that the output voltage depends also on the electrostatic force (through the membrane deflection) leads to an iterative model. As explained below, this is ignored in the first model.

4.2.2 Parabolic model

In this model, the deflection shape is assumed parabolic. The electrostatic force has the same value everywhere and is calculated with the distance h instead of using the real membrane-backplate distance. As the deflection of the membrane is supposed small, the output voltage E used for the calculation of the electrostatic force is the polarisation voltage V . The calculations lead to an output voltage which is, for sure, different from V (provided that

²This is the main idea used in the third model : the β region is split in N-1 regions corresponding to N-1 active capacitances in parallel. Ideally N tends to infinity.

the membrane has moved from its rest position). This difference is ignored in this model but will be taken into account in the next ones.

These two considerations lead to the following expression of the electrostatic force :

$$F_e = \frac{V^2 \cdot \varepsilon_0}{2 \cdot h^2} A_b = \frac{V^2 \cdot \varepsilon_0 \cdot A_b}{2 \cdot h^2} \quad (4.19)$$

The retorting force F_r can be calculated on the assumption of a parabolic deflection shape :

$$\begin{aligned} F_r &= \int_0^{R_d} 2\pi\tau \, d\left(r \frac{du}{dr}\right) \\ &= 2\pi\tau \left[r \frac{du}{dr} \right]_0^{R_d} \\ F_r &= -4\pi\tau u_0 \end{aligned} \quad (4.20)$$

The equilibrium of the forces $F_a + F_e + F_r = 0$ leads to :

$$P_a \cdot A_d + \frac{V^2 \varepsilon_0 A_b}{2 \cdot h^2} - 4\pi\tau u_0 = 0 \quad (4.21)$$

The program finds the values of u_0 that satisfy this equation; if more than one solution is found, the smallest one is chosen.

During the first step (no sound pressure) the equation is solved with $F_a = 0$. The obtained deflection is used to calculate the static capacitance C_0 . The polarisation voltage V and the stray capacitance C_p are used to determine the charge Q stored in the capacitor.

During the second step, sound pressure is applied and the equation solved. The obtained deflection is used to calculate the active capacitance C_a . The charge Q , the active capacitance C_a and the stray capacitance C_p are used to calculate the output voltage E .

The second step is repeated in order to obtain the variations of the output voltage over four periods of the sound pressure periodic signal.

4.2.3 Two-regions model

This model was originally proposed in [2]. This model makes it possible to describe the deflection of the membrane in the α region, where no electrostatic force is applied.

As in the previous model, the electrostatic pressure P_e is assumed to be everywhere the same on the β region :

$$P_e = \frac{E^2 \varepsilon_0}{2h^2} \quad (4.22)$$

This pressure and the membrane deflection are functions of the output voltage E . This means that the resulting output voltage is also a function of the voltage used for the calculations. A simple MATLAB solver (*fzero*) can be used to find the output voltage that satisfies the equations.

To simplify the notations, P will be used to designate the total pressure acting on the membrane : $P(E) = P_e(E) + P_a$.

The equilibrium of the pressures can be written

$$\frac{P}{\tau} r \, dr = - d \left(r \frac{du}{dr} \right) \quad (4.23)$$

Integrating this equation gives

$$\frac{P}{\tau} \frac{r^2}{2} = -r \frac{du}{dr} + C_1 \quad (4.24)$$

The integration constant $C_1 = 0$ because $\frac{du}{dr} \Big|_{r=0} = 0$. Then,

$$\frac{P}{2\tau} r \, dr = - du \quad (4.25)$$

Integrating this equation gives

$$\frac{P}{2\tau} \frac{r^2}{2} = -u(r) + C_2 \quad (4.26)$$

$u(r = R_b) = u_b$, then

$$C_2 = \frac{P \cdot R_b^2}{4\tau} + u_b \quad (4.27)$$

Finally the deflection $\beta(r)$ in the β region is given by,

$$\beta(r) = u(r) = \frac{P \cdot R_b^2}{4\tau} \left(1 - \frac{r^2}{R_b^2} \right) + u_b \quad (4.28)$$

The deflection of the membrane at $r = R_b$ is given by solving the α region. In [2], the author is only interested by the electrostatic deflection, meaning that no sound pressure is taken into account. It is easy to include P_a in the calculation of $\beta(r)$ as P is already independent of r , but including the sound pressure in the determination of the α region would complicate the resolution. The third model, inspired from this one, makes it easier to take the effect of the sound pressure on the α region into account : this is one of the improvements proposed by this third model.

Equation (4.23) with $P = 0$ yields,

$$d \left(r \frac{du}{dr} \right) = 0 \quad (4.29)$$

Integrating twice gives :

$$u(r) = C_1 \ln(r) + C_2 \quad (4.30)$$

As $u(r = R_d) = 0$,

$$C_2 = -C_1 \ln(R_d) \quad (4.31)$$

and

$$C_1 = R_b \left. \frac{du}{dr} \right|_{r=R_b} \quad (4.32)$$

The derivative of $u(r)$ can be obtained by differentiating equation (4.28) :

$$\left. \frac{du}{dr} \right|_{r=R_b} = \left. \frac{2r(u_b - u_0)}{R_b^2} \right|_{r=R_b} = \frac{2(u_b - u_0)}{R_b} \quad (4.33)$$

Then,

$$C_1 = 2(u_b - u_0) \quad (4.34)$$

but equations (4.31) and (4.30) lead to

$$u(r) = C_1 (\ln(r) - \ln(R_d)) \quad (4.35)$$

Finally the deflection $\alpha(r)$ in the α region is given by :

$$\alpha(r) = 2(u_b - u_0) \ln\left(\frac{r}{R_d}\right) \quad (4.36)$$

This equation makes it possible to determine the deflection u_b of the membrane at $r = R_b$:

$$\begin{aligned} u_b &= \alpha(r = R_b) \\ &= 2(u_b - u_0) \ln\left(\frac{R_b}{R_d}\right) \end{aligned} \quad (4.37)$$

Simplifying this relation gives :

$$\frac{u_b}{u_0} = \frac{2 \ln(R_d/R_b)}{1 + 2 \ln(R_d/R_b)} \quad (4.38)$$

Dividing the relation (4.28) by u_0 gives :

$$\frac{\beta(r)}{u_0} = \frac{u_0 - u_b}{u_0} \left(1 - \frac{r^2}{R_b^2}\right) + \frac{u_b}{u_0} \quad (4.39)$$

Using (4.38) and simplifying the relation leads to :

$$\frac{\beta(r)}{u_0} = \left(1 - \frac{r^2}{R_b^2}\right) \frac{1}{1 + 2 \ln\left(\frac{R_d}{R_b}\right)} \quad (4.40)$$

Likewise, using (4.38) in (4.36) divided by u_0 leads to :

$$\frac{\alpha(r)}{u_0} = \frac{2 \ln(R_d/r)}{1 + 2 \ln(R_d/R_b)} \quad (4.41)$$

The determination of u_0 is done by evaluating equation (4.28) at $r = 0$ and replacing u_b by its expression in (4.38) :

$$\beta(0) = \frac{P \cdot R_b^2}{4\tau} + u_b \quad (4.42)$$

$$u_0 = \frac{P \cdot R_b^2}{4\tau} + u_0 \frac{2 \ln(R_d/R_b)}{1 + 2 \ln(R_d/R_b)} \quad (4.43)$$

Simplifying this relation gives :

$$u_0 = \frac{P \cdot R_b^2}{4\tau} \left(1 + 2 \ln \frac{R_d}{R_b} \right) \quad (4.44)$$

Finally the active capacitance is calculated by :

$$C_a = R_s \int_0^{R_b} \frac{\varepsilon_0 \cdot 2 \cdot \pi \cdot r}{h - \beta(r)} dr \quad (4.45)$$

For the calculation of the static deflection, E is replaced in (4.22) by the polarisation voltage V and $P_a = 0$. The obtained value of C_a which is in fact the rest capacitance C_0 is used to calculate the charge Q stored in the cartridge during the polarisation process :

$$Q = V \cdot (C_0 + C_p) \quad (4.46)$$

During the calculation with sound pressure, the active capacitance is used together with the stored charge to calculate the resulting output voltage :

$$E_{out} = \frac{Q}{C_a + C_p} \quad (4.47)$$

To determine the deflection, the algorithm could be :

1. Take a starting value for E
2. Calculate the pressure $P = P_e(E) + P_a$
3. Calculate u_0 using equation (4.44)
4. Calculate u_b using equation (4.38)

5. Calculate the deflection profile using equations (4.28) and (4.36)³
6. Calculate the active capacitance using the equation (4.45)
7. Calculate the output voltage E_{out} using equation (4.47)
8. If E_{out} and E are different, take a new value of E and repeat the procedure

This is not *exactly* the way the program is operating : functions are used and the MATLAB solver *fzero* is used to find the value of E that leads to $E_{out}(E) - E = 0$.

This model has limitations that could lead to errors for soft diaphragms or high SPL :

- The electrostatic force is assumed to be everywhere the same, which is no longer valid in the case of large deflection (the force varies with the square of the deflection).
- The acoustic pressure is neglected in the α region, underestimating the membrane deflection.

4.2.4 N-regions model

This model has been developed during this master project in order to improve the existing models in the literature to larger deflections (softer diaphragms of higher SPL). As already explained, modelling the distortion (by modelling the membrane deflection profile) in such conditions requires to take the unequal distribution of the electrostatic forces into account.

To do so, the previous model is used but improved : the β region is split in $N-1$ sub-regions (N is a parameter which can be changed). On each sub- β region, an electrostatic force, function of the distance subregion-backplate, is applied. The backplate is also seen in pieces that make it possible to include dished backplate into account (see section 3.2.3).

This splitting makes the model a bit more complicated as the algorithm is not looking for only one value (previously E) but two : the output voltage and the centre deflection. As explained below, the algorithm is made of a *nested* iterative process.

An important difference between this model and the previous one is the boundary conditions used to determine the integration constants. In the

³As only the β region is necessary for the calculation of the output voltage, the α region is calculated to display the deflection profile into the GUI.

two-regions model, the derivative of the deflection at the *left*⁴ point and the deflection at the *left* point are used (see equations (4.25) and (4.27) respectively); in the following model both integration constants are found using the left point.

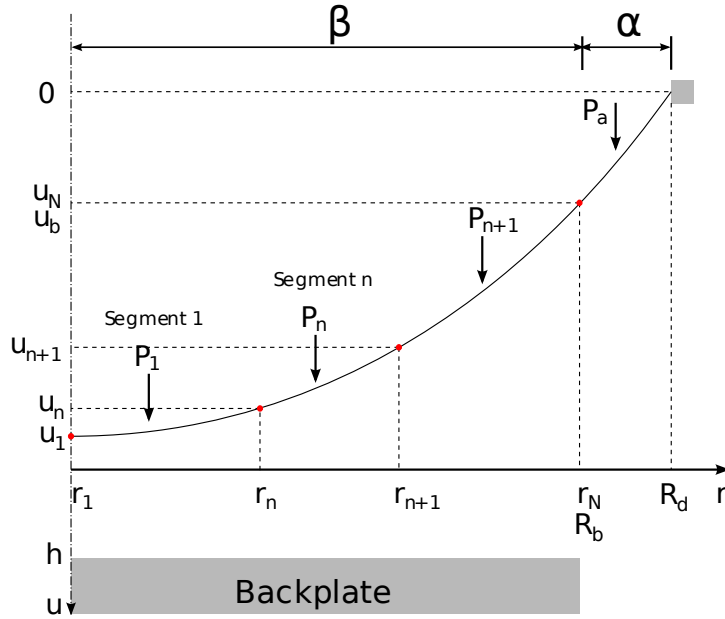


Figure 4.6: Schema of the membrane split into $N=4$ segments

First segment. The calculation of the deflection on each section of the β region is the same. The first one is a little bit different as the boundary conditions are known : at $r = 0$ the deflection is equal to u_0 and the derivative is null.

As in the previous model we have :

$$\frac{P_1}{\tau} r dr = -d \left(r \frac{du}{dr} \right) \quad (4.48)$$

but with

$$P_1 = \frac{E^2 \varepsilon}{2u_1^2} \quad (4.49)$$

A first integration leads to

$$\frac{P_1}{\tau} \frac{r^2}{2} = -r \frac{du}{dr} + A_1 \quad (4.50)$$

⁴In figure 4.6, the left point of the segment n is the point at $r = r_n$ and the right point is at $r = r_{n+1}$

The first boundary condition gives

$$\left. \frac{du}{dr} \right|_{r=0} = D_1 = 0 \quad (4.51)$$

then $A_1 = 0$. A second integration gives

$$\frac{P_1 r^2}{\tau} = -u(r) + B_1 \quad (4.52)$$

The second boundary condition $u(r = r_1) = u_1$ ⁵ gives

$$B_1 = u_1 + \frac{P_1}{4\tau} r_1^2 = u_1 \quad (4.53)$$

Finally,

$$\beta_1(r) = u(r) = -\frac{P_1}{\tau} \frac{r^2}{4} + u_1 \quad (4.54)$$

This equation shows that both E and the centre deflection u_1 are needed for the calculation. As shown in the next step, the position and the derivative of the right point are needed to continue the calculations,

$$D_2 = \left. \frac{du}{dr} \right|_{r=r_2} = -\frac{P_1}{2\tau} r_2 \quad (4.55)$$

$$u_2 = u(r_2) = u_1 - \frac{P_1}{4\tau} r_2^2 \quad (4.56)$$

The steps 2 to N are similar, the following equations are then using general notations (subscripts n and $n + 1$ to designate the left and the right points respectively).

Segment n . On the n^{th} section we have :

$$\frac{P_n}{\tau} r \, dr = -d \left(r \frac{du}{dr} \right) \quad (4.57)$$

with

$$P_n = \frac{E^2 \varepsilon}{2u_n^2} \quad (4.58)$$

A first integration leads to

$$\frac{P_n}{\tau} \frac{r^2}{2} = -r \frac{du}{dr} + A_n \quad (4.59)$$

⁵Notice that, due to the numbering from 1 to N, the centre deflection u_0 is here u_1 and the deflection at $r = R_b$ is u_N . See figure 4.6.

The first boundary condition gives

$$\left. \frac{du}{dr} \right|_{r=r_n} = D_n \quad (4.60)$$

then

$$A_n = \frac{P_n r_n^2}{\tau} + r_n \cdot D_n \quad (4.61)$$

A second integration gives

$$\frac{P_n}{\tau} \int \frac{r}{2} dr = -du + \int \frac{A_n}{r} dr + B_n \quad (4.62)$$

$$\frac{P_n r^2}{\tau} - A_n \ln(r) = -u(r) + B_n \quad (4.63)$$

The second boundary condition $u(r = r_n) = u_n$ gives

$$B_n = u_n + \frac{P_n r_n^2}{4\tau} - A_n \ln(r_n) \quad (4.64)$$

Finally,

$$\beta_n(r) = A_n \ln(r) + B_n - \frac{P_n r^2}{\tau} \quad (4.65)$$

For the next step,

$$D_{n+1} = \left. \frac{du}{dr} \right|_{r=r_{n+1}} = \frac{A_n}{r_{n+1}} - \frac{P_n}{2\tau} r_{n+1} \quad (4.66)$$

$$u_{n+1} = u(r_{n+1}) = A_n \ln(r_{n+1}) + B_n - \frac{P_n r_{n+1}^2}{\tau} \quad (4.67)$$

When all the sections have been calculated, the derivative D_N at R_b is made available. This one is used in the determination of the α region.

Taking the acoustic pressure into account, the equilibrium of the forces in the α region is given by :

$$\frac{P_a}{\tau} r dr = -d \left(r \frac{du}{dr} \right) \quad (4.68)$$

A first integration gives

$$\frac{P_a r^2}{\tau} = -r \frac{du}{dr} + C_1 \quad (4.69)$$

C_1 can be determined from the derivative and position of the point at $R_b = r_N$:

$$\begin{aligned} C_1 &= \frac{P_a r^2}{\tau} + r \left. \frac{du}{dr} \right|_{r=r_N} \\ &= \frac{P_a R_b^2}{\tau} + R_b \cdot D_N \end{aligned} \quad (4.70)$$

A second integration gives

$$\frac{P_a r^2}{\tau 4} - C_1 \ln(r) = -u(r) + C_2 \quad (4.71)$$

As $u(R_d) = 0$, we have

$$C_2 = \frac{P_a R_d^2}{\tau 4} - C_1 \ln(R_d) \quad (4.72)$$

Finally

$$\begin{aligned} \alpha(r) &= \frac{P_a R_d^2}{\tau 4} - C_1 \ln(R_d) + C_1 \ln(r) - \frac{P_a r^2}{\tau 4} \\ &= \frac{P_a}{4\tau} (R_d^2 - r^2) + C_1 \ln\left(\frac{r}{R_d}\right) \\ \alpha(r) &= \frac{P_a}{4\tau} (R_d^2 - r^2) + \left(\frac{P_a R_b^2}{\tau 2} + R_b \cdot D_N\right) \ln\left(\frac{r}{R_d}\right) \end{aligned} \quad (4.73)$$

These calculations are done in an double iterative process : the algorithm is the same as the previous model provided that the forth step (determination of u_b) is done by another iterative process.

4.3 Calculation of the output voltage and distortion

4.3.1 Output voltage

As given in equation (4.74), the microphone output voltage E depends on the three capacitances presented at the beginning of this chapter :

The active capacitance C_a is the capacitance created by the backplate and the diaphragm; it varies with the distance between these two plates and thus with the sound pressure. This capacitance is the larger one.

The static/rest capacitance C_0 is the value of the active capacitance when the microphone is not exposed to any sound pressure; the membrane is in its rest position (static deflection profile), meaning bended toward the back electrode (effect of the polarisation voltage) but without moving.

The passive capacitance C_p is the sum of all the unwanted capacitances such as the housing capacitance, the amplifier capacitance, etc.

$$E = V \frac{C_0 + C_p}{C_a + C_p} = \frac{Q}{C_a + C_p} \quad (4.74)$$

4.3.2 Distortion

The distortion in the output voltage is calculated by mean of a Fast Fourier Transform. The amplitude of the second and third harmonics are divided by the amplitude of the signal :

$$D_n(\%) = \frac{A_n}{E_{\text{eff}}\sqrt{2}} \cdot 100 \quad n = 1, 2 \quad (4.75)$$

Obtained results

In order to analyse the influence of the different causes of distortion, the results given by four models are presented. Each model takes one additional source of distortion into account. The most basic model would be made of two plates : the diaphragm and the backplate. The diaphragm would remain plane and move back and forth under the influence of the acoustic pressure and a restoring spring force. The results of this model will not be presented as it is theoretically free of distortion¹.

The first model corresponds to this basic model but taking the stray capacitances into account. Then, the parabolic deflection of the membrane and the electrostatic forces are added successively :

Model 1 The diaphragm remains plane and moves back and forth under the influence of the acoustic pressure and a restoring spring force. Stray capacitances are taken into account (load, edge and housing capacitances).

Model 2 The deflection of the diaphragm is assumed parabolic (fixed on the edges).

Model 3 The electrostatic force is applied on the membrane. The force is constant in time and equal everywhere to the force calculated with the distance h .

¹This basic model has nevertheless been modelled and the algorithm tested : the calculated distortion, which varies randomly with the sound pressure level, is equal to -300 dB at 140 dB SPL. This probably corresponds to the noise floor of the Fast Fourier Transform calculation.

Model 4 The accuracy of the model is improved : the electrostatic force depends on the deflection of the membrane and thus on the position along the membrane. The membrane deflection is then free to take a more realistic shape.

5.1 Simulated microphones

Six Brüel & Kjær microphones have been modelled; the different parameters needed for the simulation have been measured from the construction drawings². The distance h between the backplate and the diaphragm has been adjusted ‘manually’ in order to get the right sensitivity at 93.98 dB SPL (1 Pa). The equivalent volume of the diaphragm V_d is never modified in order to keep the same mechanical properties of the microphone.

Two of the six microphones have been selected to present the results. The 4190 is a standard 1/2” sound level microphone, the 4179 is a low-noise 1” sound level microphone. A low-noise microphone, which is characterised by a very soft diaphragm and thus a very low noise floor (the 4179 noise floor is -2.5 dB(A) [27, 12]), makes it possible to measure very low sound pressure levels.

5.1.1 Microphones data

The parameters³ of the two selected microphones are given in table 5.1. The data for the six microphones are available in the microphone library of the simulation program.

5.1.2 Equivalent volume of the diaphragm

The equivalent volume of the diaphragm V_d is a useful quantity, it is the volume of air which has a mechanical compliance equal to the one of the diaphragm. It makes it possible to know either the diaphragm or the back-volume is the dominant factor in the system total compliance. When V_d is not directly available, it can be calculated from the tension and thickness of the diaphragm and the volume of the back cavity using the equation (5.1).

²The values of the housing capacitance C_h and equivalent volume of the diaphragm V_d have been measured and given by the manufacturer.

³The values of h correspond to the ones adjusted for the fourth model

Parameter	4190	4179
R_d (mm)	4.6	8.9
R_b (mm)	3.45	6.65
A_h (mm ²)	3.96	42.98
W_b (μ m)	800	650
L_e (mm)	48.1	268
C_l (pF)	0.2	0.2
C_h (pF)	1.65	1.5
V_d (mm ³)	48.085	400
h (μ m)	26.787	32.082
S_c (mV/Pa)	50	100

Table 5.1: Parameters used for the simulation of the B&K microphones

$$\begin{aligned}
V_d &= \rho c^2 C_{ad,eq} \\
&= \rho c^2 \left(\frac{1}{C_{ad}} + \frac{1}{C_{ab}} \right)^{-1} \\
&= \rho c^2 \left(\frac{R_d^4}{8\tau} + \frac{\rho c^2}{V_b} \right)^{-1} \\
V_d &= \rho c^2 \left(\frac{R_d^4}{8\sigma t_d} + \frac{\rho c^2}{V_b} \right)^{-1} \tag{5.1}
\end{aligned}$$

Where ρ is the air density, c the speed of sound in the air, $C_{ad,eq}$ the total equivalent acoustic compliance of the diaphragm (including the effect of the back volume), C_{ad} the acoustic compliance of the diaphragm alone, V_b the volume of the back cavity and σ membrane tensile stress (usually expressed in MPa).

This calculation has been done for the microphone 4955 as only $\sigma=100$ MPa, $t_d=2$ μ m and $V_b=618$ mm³ where given. The obtained result was :

$$\begin{aligned}
V_d &= 1.204 \times 344^2 \times \left(\frac{(4.5 \cdot 10^{-3})^4}{8 \times 100 \cdot 10^6 \times 2 \cdot 10^{-6}} + \frac{1.204 \times 344^2}{618 \cdot 10^{-9}} \right)^{-1} \\
&= 618 \text{ mm}^3
\end{aligned}$$

In the first model, the restoring spring force is calculated from the equivalent volume of the diaphragm by :

$$F_r = -k u_0 \tag{5.2}$$

where k is the spring constant defined by :

$$k = \frac{1}{C_{md}} = \frac{A_d^2}{C_{ad}} = \frac{\rho c^2 A_d^2}{V_d} \quad (5.3)$$

C_{md} and A_d are respectively the mechanical compliance of the diaphragm and its area.

For the other models, the tension τ is used. It is calculated from the relation :

$$\tau = \frac{\pi R_d^4}{8 C_{ad,eq}} = \frac{\rho c^2 \pi R_d^4}{8 V_d} \quad (5.4)$$

This relation (already used in equation (5.1)) is only valid for a parabolic deflection profile of the diaphragm. As the fourth model is not based on a parabolic profile but lets the membrane free to take its natural profile, this value of the membrane tension introduces errors in the calculations with this final model. However, it is assumed that the error on the tension is negligible and does not influence the distortion result too much.

5.1.3 Adjustment of the model sensitivity

Changing the model (or any parameter) changes the sensitivity of the microphone. Thus, the distance h has to be adjusted everytime a parameter is changed. It is important to “calibrate” the model as it makes it possible to compare the distortion results. The table 5.2 gives the values of h that should be used for each model in order to have a sensitivity of 50 mV/Pa and 100 mV/Pa at 93.98 dB SPL for the 4190 and the 4179 respectively.

Microphone	Model 1	Model 2	Model 3	Model 4
4190	17.502 μm	24.055 μm	25.310 μm	26.787 μm
4179	19.790 μm	27.565 μm	29.632 μm	32.082 μm

Table 5.2: Distance membrane backplate h used to obtain the correct sensitivity

5.2 Predicted membrane deflection profile

5.2.1 Standard microphone B&K 4190

The figure 5.1 shows the membrane deflections of a microphone B&K 4190 exposed to 140 dB SPL, calculated by the four models. The black curves represent the static deflections (when the acoustic pressure is null), the red

and blue curves represent the deflections when the acoustic pressure is respectively minimal and maximal. These two curves are the two extreme positions of the membrane. The deflections are expressed in fraction of the air-gap thickness, positive values on the backplate side (the collapse occurs when the normalised deflection equals 1).

The influence of the electrostatic force (which is present in models 3 and 4) can be seen on the two lower graphs : the static deflection is positive and the displacement of the membrane is larger on the backplate side.

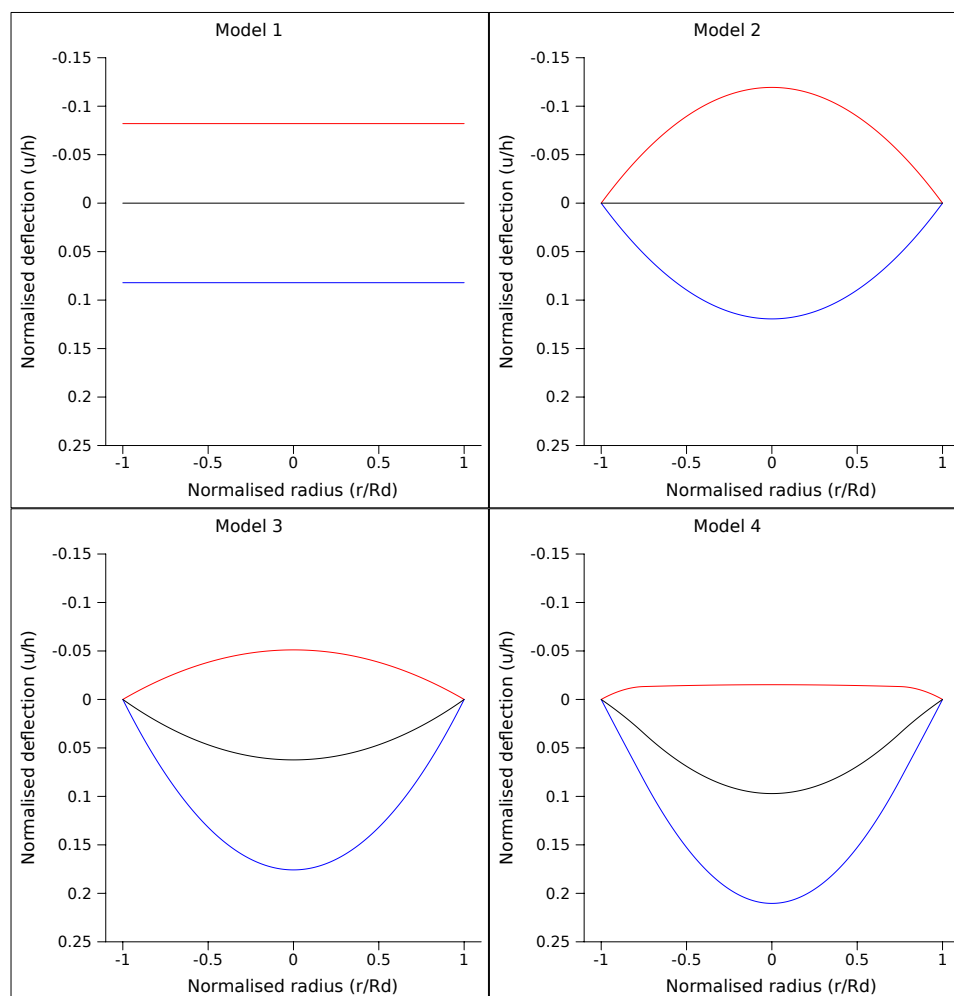


Figure 5.1: Predicted deflection of the microphone B&K 4190 exposed to 140 dB SPL

The peak-peak displacements of the membrane at its centre, for the different models, are listed in table 5.3.

As one can see, the peak-peak distance at the centre for the model 2 is exactly two times the one for the model 1; this has to be related to the volume of air a parabolic profile and a plane profile move.

Let us consider a flat diaphragm of radius R_d having a displacement u_0 , the volume V_f displaced by the flat diaphragm is :

$$V_f = \pi R_d^2 u_0 \quad (5.5)$$

while the volume V_p displaced by a parabolic diaphragm is :

$$\begin{aligned} V_p &= \int_0^{R_d} 2\pi r u_0 \left(1 - \left(\frac{r}{R_d}\right)^2\right) dr \\ &= 2\pi u_0 \int_0^{R_d} \left(r - \frac{r^3}{R_d^2}\right) dr \\ &= 2\pi u_0 \left[\frac{r^2}{2} - \frac{r^4}{4R_d^2}\right]_0^{R_d} \\ &= \frac{\pi R_d^2 u_0}{2} \\ V_p &= \frac{V_f}{2} \end{aligned} \quad (5.6)$$

The diaphragm having the same equivalent volume in both models, the volume it displaces is the same for an equal applied acoustic pressure. Thus, in the second model the centre displacement of the membrane should be two times larger than the displacement of the membrane in the first model in order to move the same volume of air.

The diaphragm movement is as wide in the second and in the third model because the electrostatic force is constant. This force moves the rest position of the membrane but has no influence on the amplitude of its movement.

The membrane displacement in model 4 is the largest, it is probably due to the electrostatic force which is more important. This explanation is probably valid for the lower deflection (blue curve) because the distance membrane-backplate is smaller than h (distance used in model 2 to calculate the electrostatic forces) and thus the force larger. However this explanation does not stand for the upper deflection : the movement of the membrane in the opposite direction (red curve) is reduced, while the electrostatic force is now weaker (distance larger than h).

5.2.2 Low noise microphone B&K 4179

The deflection results obtained with the low noise microphone are given in table 5.4. Comparing these results to the ones obtained with the 4190, one

Model 1	Model 2	Model 3	Model 4
2.87 μm	5.74 μm	5.74 μm	6.04 μm

Table 5.3: Peak-peak deflection value of the B&K 4190 at 140 dB SPL

can see that the deflection are larger with the 4179, probably because the diaphragm of the 4179 is softer.

Model 1	Model 2	Model 3	Model 4
6.38 μm	12.76 μm	12.76 μm	13.70 μm

Table 5.4: Peak-peak deflection value of the B&K 4179 at 140 dB SPL

5.3 Predicted sensitivity

5.3.1 Standard microphone B&K 4190

In addition to the distortion, the sensitivity of the cartridge is also calculated at different sound pressure levels. As one can see in figure 5.2, the sensitivity of the microphone B&K 4190 remains constant at 50 mV/Pa (-26 dB re 1V/Pa) below 130 dB SPL and increases up to 52.16 mV/Pa (-25.7 dB) at 154 dB SPL for the fourth model. This increasing in sensitivity occurs above 130 dB SPL for the B&K 4190, no matter the model used. More complex the model, more important the change in sensitivity. Moreover, the model without any stray capacitance (which is, then, free of distortion) does not give any variation in sensitivity. This phenomenon has not been mentioned in any document of the bibliography. The measurement of the sensitivity of a microphone exposed to high sound pressure levels would make it possible to determine if this increasing is real or due to errors in the model.

5.3.2 Low noise microphone B&K 4179

The variations of microphone B&K 4179 sensitivity is presented in figure 5.3. Again, an increase of sensitivity is observed; the variation is comparable with the one of the B&K 4190 in its shape. However, the increase is slightly less important here : +3.34% compared to +4.31% for the B&K 4190.

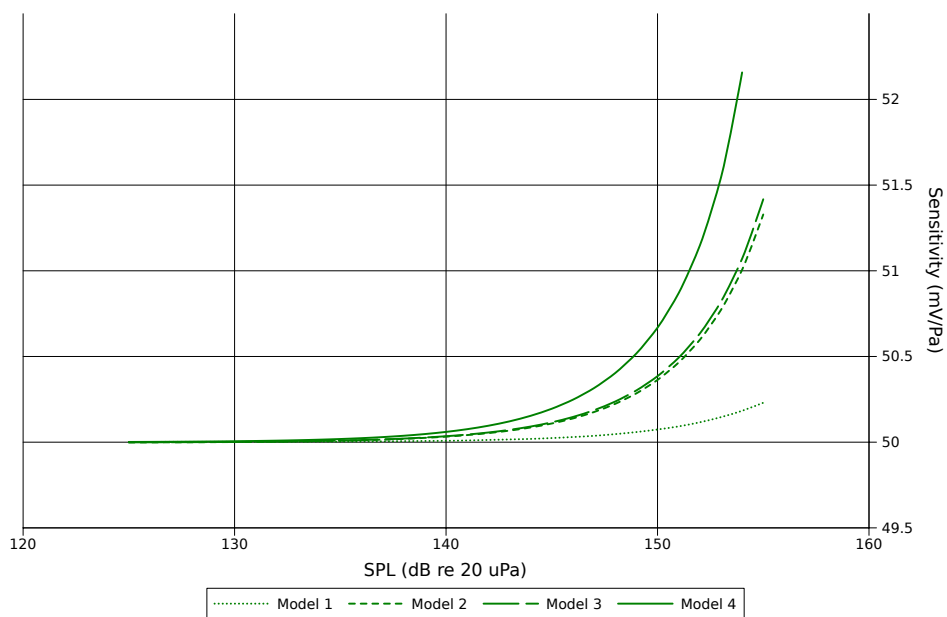


Figure 5.2: Predicted sensitivity of the microphone B&K 4190

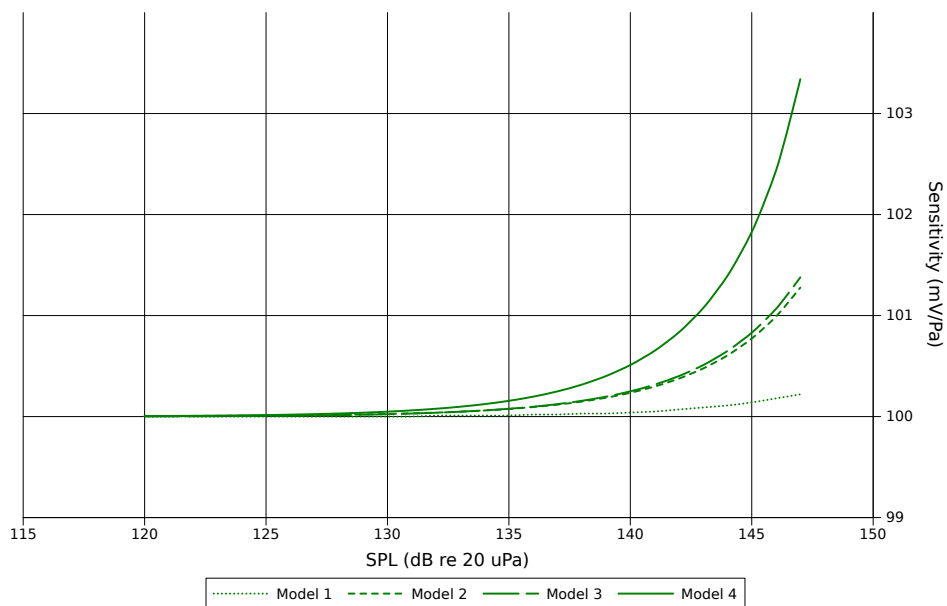


Figure 5.3: Predicted sensitivity of the microphone B&K 4179

5.4 Predicted distortion

5.4.1 Standard microphone B&K 4190

The second and third harmonic distortion (D_2 and D_3 respectively) have been calculated with the different models. This makes it possible to see how much each source of distortion increases the overall distortion. The distortion level of the microphone B&K 4190 is represented in figure 5.4 as a function of the sound pressure level.

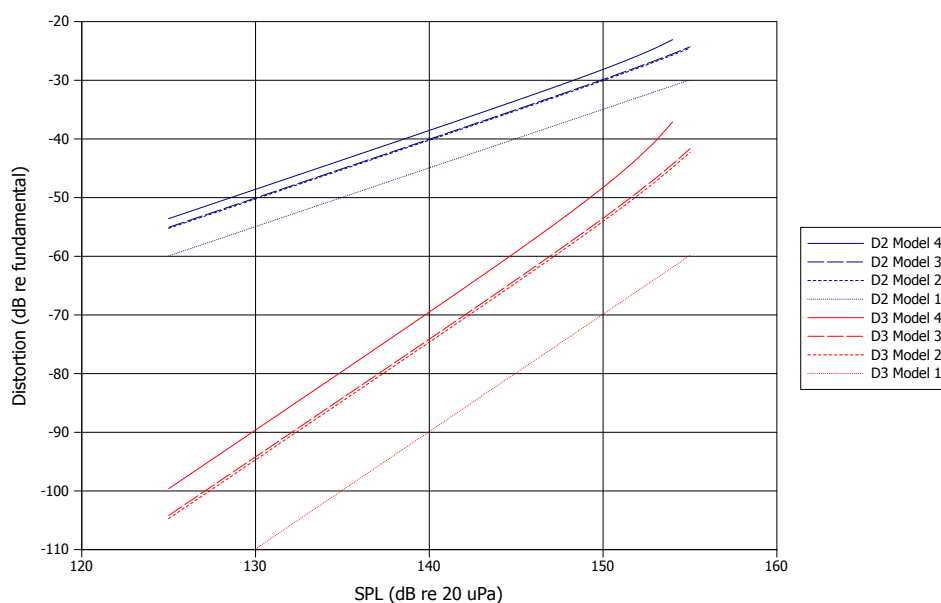


Figure 5.4: Predicted distortion of the microphone B&K 4190

Model	D_2 @ 140 dB SPL (dB)	D_3 @ 140 dB SPL (dB)
1	-44.93	-89.87
2	-40.21	-74.64
3	-40.04	-74.12
4	-38.55	-69.50
Manufacturer [1]	-40.9	-66.0

Table 5.5: Influence of the model on the distortion results (B&K 4190)

As one can see on the graph, the difference between the results given by the different models is only a vertical shift of the curves. The table 5.5 gives the calculated distortion values given by each model at 140 dB SPL (sound

pressure level chosen arbitrary).

The increasing of the distortion with the model observed in figure 5.4 and table 5.5 agree with the deflection figures 5.1. As one can see on the deflection figures, the displacement on the outer regions of the diaphragm is getting smaller with the complexity of the model. These regions can be seen as weakly active capacitances or even *quasi-passive* capacitances. These capacitances load the most active regions and thus increase the distortion.

The influence of the deflection shape can be evaluated by comparing the second harmonic distortion levels of the model 1 (flat diaphragm) and the model 2 (parabolic diaphragm). For the 4190, the parabolic shape increases the distortion by approximately 4.7 dB. This increasing due to the non planar deflection shape reaches approximately 6.4 dB when the the deflection shape is improved by the last model (comparing models 1 and 4).

5.4.2 Low noise microphone B&K 4179

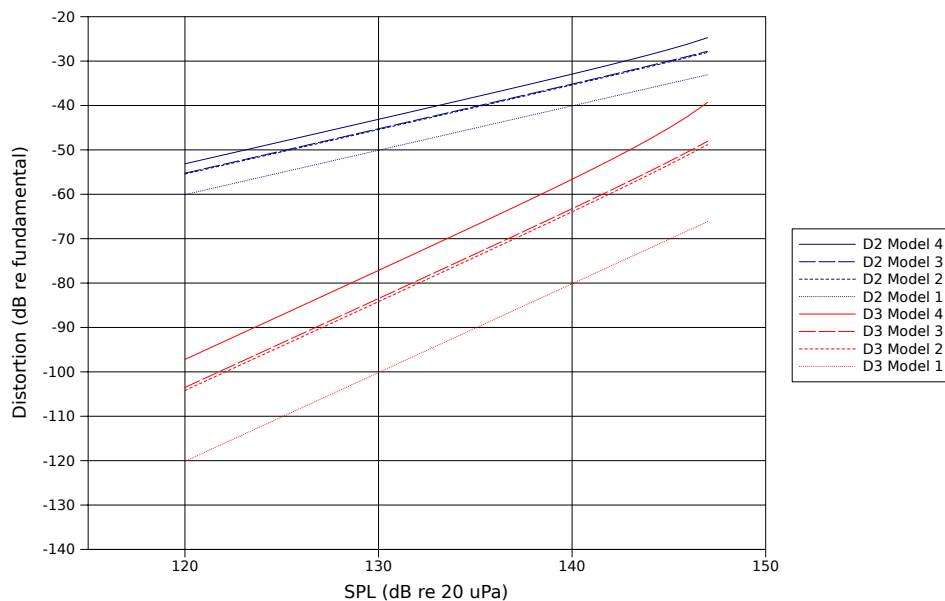


Figure 5.5: Simulated distortion for the microphone B&K 4179

For this microphone the effect of the parabolic shape is an increase of the second harmonic distortion by approximately 4.7 dB. The real deflection shape leads to an increase of approximately 7.2 dB.

It appears that the increase of distortion due to the parabolic shape is the same for both microphones but the true deflection shape leads to a larger in-

Model	D_2 @ 140 dB SPL (dB)	D_3 @ 140 dB SPL (dB)
1	-40.08	-80.15
2	-35.37	-63.95
3	-35.17	-63.25
4	-32.93	-56.62
Manufacturer [27]	-30.46	N/A

Table 5.6: Influence of the model on the distortion results (B&K 4179)

creasing of distortion for the low-noise microphone. It can be concluded that the last model has a larger influence on the results for the soft diaphragm microphone. The predictions are probably better for a low-noise microphone when the fourth model is used.

5.5 Influence of the diaphragm and backplate radius ratio on the distortion

As explained in section 3.6.3.2, the optimum ratio between the backplate radius R_b and the diaphragm radius R_d is derived in [2]. The calculation leads to an optimum ratio of $(2/3)^{1/2} \approx 0.8165$.

The variation of the second harmonic distortion in a microphone B&K 4190 has been simulated as a function of the ratio R_b/R_d using the most advanced model (model 4). The results obtained at 140 dB SPL are shown in figure 5.6 (the green dot corresponds to the optimum ratio cited above, the red one corresponds to the optimum ratio found by the model). As one can see, the optimum value for which the distortion is minimum is found at $R_b/R_d = 0.75$. This ratio is the actual ratio for this microphone (see table 5.1). The difference between this value and the theoretical one given in [2] can be explained by the presence of holes in the backplate. These holes, needed to control the damping of the system, reduce the active backplate area; they are not taken into account in the theoretical calculations proposed in [2].

5.6 Reducing distortion

As explained in the theory section 3.2.3, it is theoretically possible to reduce the distortion by using a curved backplate. The curvature of the backplate compensates for the deflection profile of the diaphragm. According to the previous results, the curved shape of the diaphragm deflection is responsible for about 5 dB of distortion. It is then expected that the maximum reduction

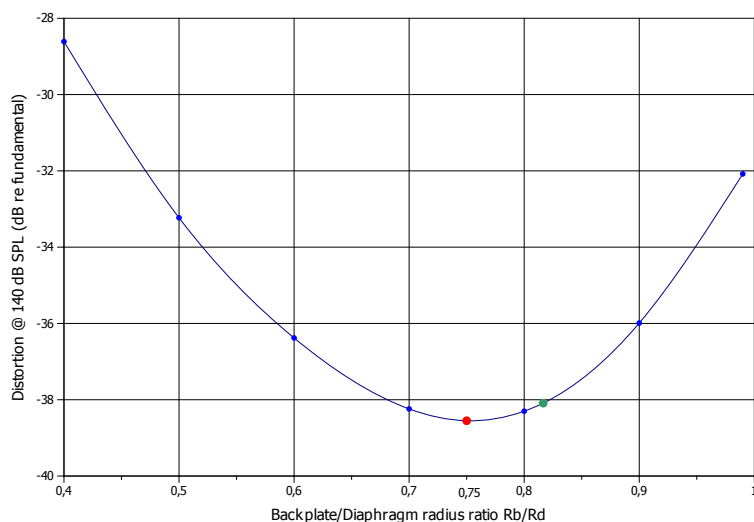


Figure 5.6: Influence of the backplate radius on the distortion (B&K 4190)

this improvement can make is about 5 dB. Indeed, it is impossible to adjust the backplate curvature to match exactly the one of the diaphragm, since this profile changes with the time and the sound pressure level.

Even if a spherical curvature is only a raw approximation of the membrane deflection shape, a so curved backplate gives a satisfactory reduction of the distortion. The figure 5.7 shows the influence of the backplate curvature radius on the distortion of a microphone B&K 4190. According to this figure, the optimum radius of curvature for this microphone is 275 mm. This optimum is the same at 130, 140 and 150 dB SPL but leads to different reductions of the distortion : respectively 4.18, 4.21 and 4.62 dB. It would have been interesting to calculate this reduction of distortion at other levels, but these levels are already promising and fit with the expected results.

It also appears that the distortion increases rapidly when the radius of curvature is reduced below the optimal one. The reason of this increase is probably that the outer regions, which are less active because they do not move as much as the centre regions, gain in capacitance as the distance to the backplate is reduced. As already explained in section 5.4.1, these weakly active regions behave as an (almost) passive capacitance loading the active one : the distortion increases.

Figure 5.8 makes it possible to determine which way is the best to increase the sensitivity of the microphone B&K 4190 without increasing too much the distortion (or decrease the distortion without losing too much sensitivity). The following observations are probably true for other condenser microphones.

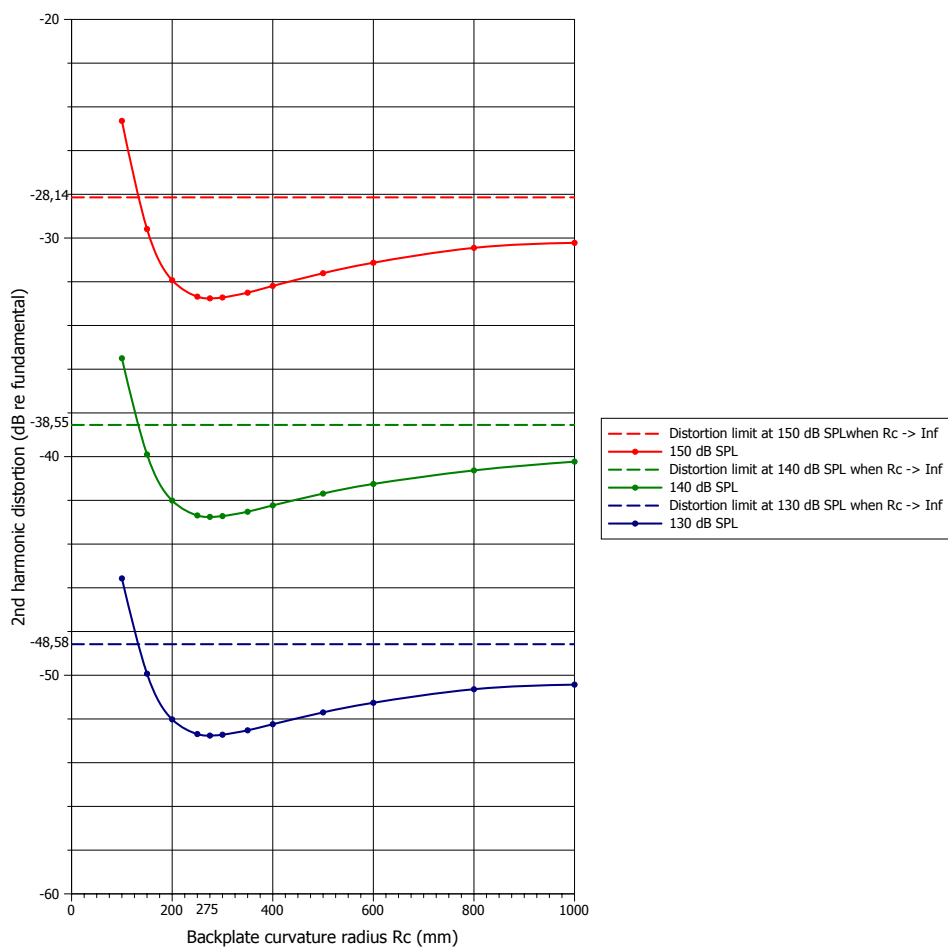


Figure 5.7: Influence of the backplate curvature radius on the distortion (B&K 4190)

Two groups of two curves are shown on this figure. The first group corresponds to a normal B&K 4190 with the specifications given in table 5.1. The second group corresponds to the same microphone but with a curved backplate; the optimum radius of 275 mm determined above is used.

Two means of changing the sensitivity are considered here : changing the polarisation voltage V (red curves) or changing the distance membrane-backplate h (blue curves). The intersection points between the blue and the red curves correspond to a standard working point : a microphone polarised at 200 V having a sensitivity of 50 mV/Pa (-26 dB re 1V/Pa) at 140 dB SPL.

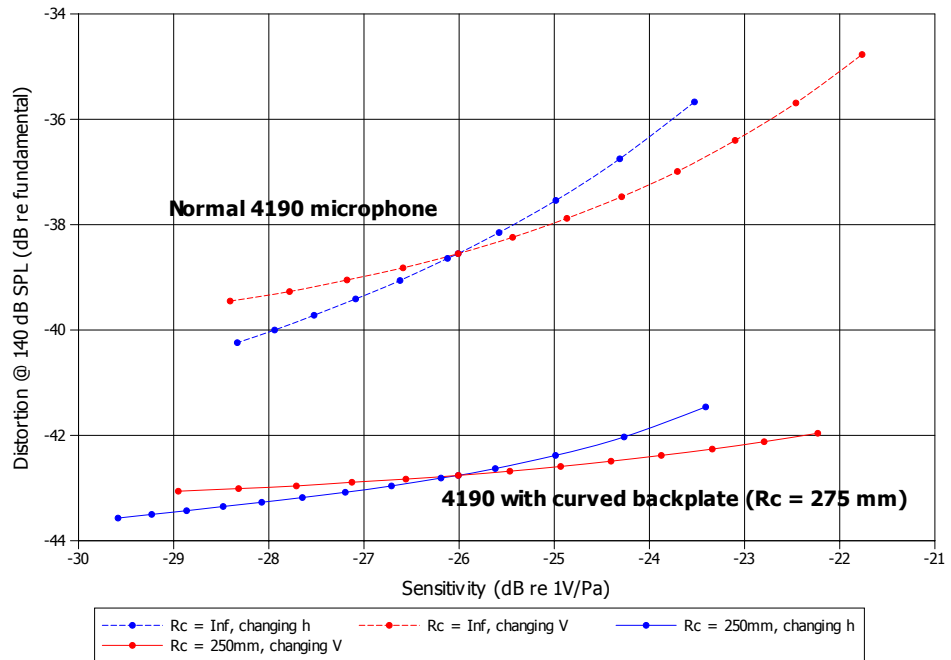


Figure 5.8: Influence of V , h and R_c on the distortion (B&K 4190)

A first general observation is that the blue curves grow more rapidly than the red ones. This leads to two remarks :

- Increasing the sensitivity should be done by increasing the polarisation voltage V (following the red curve towards the right). This makes the increase of distortion smaller compared to the method that consist in reducing the air-gap thickness h (following the blue curve towards the right).
- Reducing the distortion should be done by increasing h (following the

blue curve towards the left). Trying to reduce the distortion by reducing the polarisation voltage leads to a more important loss in sensitivity.

As one can see comparing the two sets of curves, the curves slopes are more gentle for the curved backplate design.

- The increase of sensitivity by increasing the polarisation voltage leads to a smaller increase in distortion compared to the normal microphone.
- Even if increasing h is still the better solution to reduce the distortion, the loss in sensitivity is more important compared to the normal backplate design.

It can be concluded that beside reducing the general distortion levels, the curved backplate design enables to increase the sensitivity of a microphone without increasing the distortion too much.

Perspectives

The model developed during this study enables to model the displacement of the membrane of any common externally polarised condenser microphone. This model is a low frequency and quasi-static model taking the variations of the electrostatic forces into account.

This model makes it possible to simulate the effect of advanced backplate shapes, promising results have been given in the previous chapter.

This model has been good enough to evaluate the influence of the membrane deflection profile on the distortion but it can be improved in many ways and could then be used for other studies :

1. A first improvement could be the possibility to model electret microphones. This would lead to the study of the charge mobility in the electret layer and maybe to a better understanding of the capacitance and thus of the charge distribution along the membrane.
2. Then the model could be turned into a dynamic model that takes the mass of the membrane into account. This would make it possible to simulate the system frequency response.
3. The next step would be to consider the vibration modes of the diaphragm in order to make improve the prediction at high frequencies.

On the other hand, the simulation program could be improved on the following points :

1. First, a function that adjusts automatically the distance membrane-backplate h in order to get the correct microphone sensitivity would be a useful improvement. This would save a lot of time when comparing the influence of different microphone parameters or backplate designs on the distortion.
2. Then, it would certainly be interesting to have more informations about the ratio between the active and passive capacitances. How much the different regions of the membrane are active would also inform the user on the repartition of the active capacitances.
3. Like the other models, the forth one is based on an iteration process. This process ends when the variation of the microphone output voltage between two iterations is sufficiently low. This stop criterion is not optimised and can lead to erroneous results at low sound pressure levels, mainly on the third harmonic distortion. This phenomenon of increasing distortion when the level of the signal decreases can be compared to the cross-over distortion in push-pull amplifier : the ratio between the error and the amplitude of the output voltage increases and creates mainly third harmonic distortion.

Conclusion

This study made it possible to get a better understanding of the different causes of electrical distortion in condenser microphones. The two most important causes of distortion, the presence of stray capacitances and the curved deflection shape of the diaphragm; have been presented and simulated.

A model of membrane deflection found in the literature has been improved and developed for the needs of this study. This new model makes it possible to obtain a better estimation of the deflection shape without forcing this one to follow a parabolic curvature. This new model is more suitable to model distortion produced by low-noise microphones because of their softer diaphragm.

Finally, this model makes it possible to investigate the effect of advanced backplate profiles. A solution to reduce distortion based on a curved backplate design has been found in the literature. This solution has been simulated with the model and promising results have been found.

Bibliography

- [1] Brüel & Kjær, Nærum, Denmark. *Technical documentation - Microphone handbook for the Falcon Range of Microphone Products*, February 1995. Online documentation BE 5105-12 on <http://www.bksv.com>.
- [2] George S. K. Wong and Tony F. W. Embleton, editors. *AIP Handbook of Condenser Microphones*. AIP Press, 1995.
- [3] Brüel & Kjær, Nærum, Denmark. *Technical documentation - Microphone handbook*, July 1996. Online documentation BE 1447-11 on <http://www.bksv.com/doc/be1447.pdf>.
- [4] Erling Frederiksen. *Handbook of Signal Processing in Acoustics*, volume 2, chapter 65, pages 1247–1266. Springer, 2008.
- [5] Elmer L. Hixson and Ilene J. Busch-Vishniac. *Encyclopedia of Acoustics*, volume 4, chapter 159, pages 1889–1902. John Wiley & Sons, Inc, 1997.
- [6] Svetislav V. Djuric. Distortion in microphones. In *1976 IEEE International Conference on Acoustics, Speech and Signal Processing*, pages 537–539, 1976.
- [7] David Josephson. Nonlinearities in condenser microphone electronics - design considerations for new solid-state microphones. *AES Convention*, **89**, 1990.
- [8] Brüel & Kjær, Nærum, Denmark. *Product Data - Falcon Range 1/2" Microphone Preamplifier - Type 2669*, September 1996. Online documentation BP 1422-13 on <http://www.bksv.com/doc/bp1422.pdf>.
- [9] Holger Pastillé. Electrically manifested distortions of condenser microphones in audio frequency circuits. *J. Acoust. Soc. Am.*, **48**(6):559–563, June 2000.

- [10] Erling Frederiksen. Reduction of non-linear distortion in condenser microphones by using negative load capacitance. In *Technical Review*, volume 1, pages 13–31. Brüel & Kjær, Nærum, Denmark, 1996. Online documentation BV 0048-11 on <http://www.bksv.com/doc/bv0048.pdf>.
- [11] N.H. Fletcher and S. Thwaites. Electrode surface profile and the performance of condenser microphones. *J. Acoust. Soc. Am.*, **112**(6):2779–2785, December 2002.
- [12] Brüel & Kjær, Nærum, Denmark. *Product Data - 1/2" Low-noise Free-field TEDS Microphone - Type 4955*, September 2006. Online documentation BP 2148-11 on <http://www.bksv.com/doc/bp2148.pdf>.
- [13] Erling Frederiksen. Prepolarised condenser microphones for measurement purposes. In *Technical Review*, volume 4, pages 3–26. Brüel & Kjær, Nærum, Denmark, 1979.
- [14] Muhammad Taher Abuelma'atti. Harmonic distortion in electret microphones. *Applied Acoustics*, **34**:1–6, 1991.
- [15] P.R. Scheeper, W. Olthuis, and P. Bergveld. Improvement of the performance of microphones with a silicon nitride diaphragm and backplate. *Sensors and Actuators A*, **40**:179–186, 1994.
- [16] Michael Pedersen, Wouter Olthuis, and Piet Bergveld. Harmonic distortion in silicon condenser microphones. *J. Acoust. Soc. Am.*, **102**(3):1582–1587, September 1997.
- [17] P.R. Scheeper, A.G.H. van der Donk, W. Olthuis, and P. Bergveld. A review of silicon microphones. *Sensors and Actuators A*, **44**:1–11, 1994.
- [18] Muhammad Taher Abuelma'atti. Large signal performance of micro-machined silicon microphones. *Applied Acoustics*, **68**:616–627, 2007.
- [19] Pierre Bernard. *Microphone Intermodulation Distortion Measurements using the High Pressure Microphone Calibrator Type 4221*. Brüel & Kjær, Nærum, Denmark, 1980. Online documentation BE 083-80 on <http://www.bksv.com/doc/083-80.pdf>.
- [20] Erling Frederiksen. System for measurement of microphone distortion and linearity from medium to very high levels. In *Technical Review*, volume 1, pages 25–38. Brüel & Kjær, Nærum, Denmark, 2002.
- [21] Erling Frederiksen. *Verification of High-pressure Linearity and Distortion of Measurements Microphones*. Brüel & Kjær, Nærum, Denmark, 2004.

-
- [22] Martin Dadic. Numerical determination of electric field forces and capacitance of pressure condenser microphone. *IEEE Transactions on Instrumentation and Measurement*, **51**(6):1200–1203, December 2002.
- [23] Wikipedia. Nodal analysis, 2009. Article available on http://en.wikipedia.org/wiki/Nodal_analysis.
- [24] Jen-Yi Chen, Yu-Chun Hsu, Shu-Sheng Lee, Tamal Mukherjee, and Gary K. Fedder. Modeling and simulation of a condenser microphone. *Sensors and Actuators A*, **145–146**:224–230, 2008.
- [25] Michal Vlk. Condenser microphone as parametric electroacoustic system and its time-domain modelling via equivalent electrical circuit in spice software, June 2008.
- [26] Michal Vlk. A novel analogy for time-domain simulation of the nonlinear electrostatic transducer. In *POSTER 2008, Prague*, May 2008.
- [27] Brüel & Kjær, Nærum, Denmark. *Product Data - Condenser Microphone - Type 4179*. Online documentation BP 0389-12 on <http://www.bksv.com/doc/bp0389.pdf>.

www.elektro.dtu.dk

Department of Electrical Engineering
Centre for Electric Technology (CET)
Technical University of Denmark
Ørsteds Plads
Building 348
DK-2800 Kgs. Lyngby
Denmark
Tel: (+45) 45 25 38 00
Fax: (+45) 45 93 16 34
Email: info@elektro.dtu.dk